



**Flanders**  
State of  
the Art

17\_026\_1  
FHR reports

# Manning's roughness coefficient in SWASH

Application to overtopping calculation

DEPARTMENT  
MOBILITY &  
PUBLIC  
WORKS

[www.flandershydraulicsresearch.be](http://www.flandershydraulicsresearch.be)

# Manning's roughness coefficient in SWASH

## Application to overtopping calculation

Suzuki, T.; Altomare, C.; De Roo, S.; Vanneste, D.; Mostaert, F.

### Legal notice

Flanders Hydraulics Research is of the opinion that the information and positions in this report are substantiated by the available data and knowledge at the time of writing.  
 The positions taken in this report are those of Flanders Hydraulics Research and do not reflect necessarily the opinion of the Government of Flanders or any of its institutions.  
 Flanders Hydraulics Research nor any person or company acting on behalf of Flanders Hydraulics Research is responsible for any loss or damage arising from the use of the information in this report.

### Copyright and citation

© The Government of Flanders, Department of Mobility and Public Works, Flanders Hydraulics Research 2018  
 D/2018/3241/163

This publication should be cited as follows:

**Suzuki, T.; Altomare, C.; De Roo, S.; Vanneste, D.; Mostaert, F.** (2018). Manning's roughness coefficient in SWASH: Application to overtopping calculation. Version 2.0. FHR Reports, 17\_026\_1. Flanders Hydraulics Research: Antwerp.

Reproduction of and reference to this publication is authorised provided the source is acknowledged correctly.

### Document identification

Customer:	Agentschap Maritieme Dienstverlening en Kust, Afdeling Kust	Ref.:	WL2018R17_026_1
Keywords (3-5):	SWASH; bottom friction; wave run-up		
Text (p.):	36	Appendices (p.):	17
Confidentiality:	<input checked="" type="checkbox"/> Yes	Released as from:	01/01/2020
		Exception:	<input checked="" type="checkbox"/> The Government of Flanders

Author(s)	Suzuki, T.; Altomare, C.; De Roo, Sieglien
-----------	--

### Control

	Name	Signature
Reviser(s):	Vanneste, D.	
Project leader:	Suzuki, T.	

### Approval

Head of Division:	Mostaert, F.	
-------------------	--------------	--

## Abstract

The wave overtopping calculation method for the Safety assessment 2015 was defined in Suzuki et al. (2016). In order to get a conservative overtopping value for the safety assessment, the Manning's roughness coefficient  $n$  in the SWASH 1D overtopping calculation was deliberately set as zero. This choice however impacts the estimation of wave overtopping over a cross shore profile which includes a foreshore having a 'dry beach' part in front of the dike. Normally, a sandy beach should add dissipation to wave propagation because of its roughness. Being excluded in the aforementioned methodology, this leads to an overestimation of wave overtopping. In this study, the bottom friction parameter in SWASH is further explored for overtopping calculation under a condition with long berm (e.g. 50 m) in front of the dike.

After the study it has been concluded that material based  $n$  value gives good estimation for wave transformation and run-up, for all the tested cases. Taking into account the fact that the Manning coefficient  $n$  for the sand and promenade material would be around 0.019, and therefore the default bottom friction value  $n=0.019$  is recommended for overtopping calculation in SWASH.



# Contents

Abstract .....	III
Contents .....	V
List of tables.....	VII
List of figures .....	VIII
1 Introduction.....	1
2 Literature review .....	2
3 Data screening.....	4
3.1 Description of available datasets .....	4
3.2 Discussions and conclusions.....	13
4 Model.....	14
4.1 SWASH model.....	14
4.2 Bottom friction approaches in SWASH.....	15
4.3 Manning approach .....	15
4.3.1 Manning coefficient.....	15
4.3.2 Scaling.....	17
5 In-depth analysis of bottom friction settings in SWASH .....	18
5.1 Wenduine .....	18
5.1.1 Test cases.....	18
5.1.2 Results .....	19
5.2 Chen.....	20
5.2.1 Test cases.....	20
5.2.2 Results .....	20
5.3 ICODEP.....	22
5.4 WaLoWa .....	23
5.4.1 Test cases.....	23
5.4.2 Results .....	24
5.5 Park & Cox .....	29
5.5.1 Model settings.....	29
5.5.2 Implementation of time dependent wave run-up value in SWASH .....	30
5.5.3 Post-processing of wave run-up calculation results.....	31
5.5.4 Results .....	32

5.6 Further discussion of Fielder et al. (2018)..... 34

6 Conclusions..... 35

6.1 Bottom friction n value..... 35

6.2 Wave generation and number of waves ..... 35

References..... 36

Appendix A: WaLoWa SWASH results ..... A1

Bi\_01\_4..... A1

Bi\_01\_5..... A2

Bi\_01\_6..... A3

Bi\_02\_4..... A4

Bi\_02\_5..... A5

Bi\_02\_6..... A6

Bi\_02\_6\_R..... A7

Bi\_01\_6\_R..... A8

Bi\_03\_6..... A9

Bi\_03\_6\_1..... A10

Bi\_03\_6\_2..... A11

Appendix B: Test case calculation ..... A12

Cross section 233 (XB raai 140) ..... A12

Cross section 234 (XB raai 145) ..... A15

## List of tables

Table 3-1: Available dataset for the calibration of bottom friction in SWASH.....	4
Table 3-2: Details of SCANDURA project .....	5
Table 3-3: Details of SUSCO project .....	6
Table 3-4: Details of WISE project .....	7
Table 3-5: Details of ICODEP project .....	8
Table 3-6: Details of WALOWA project .....	9
Table 3-7: Details of CHEN project .....	10
Table 3-8: Details of Wenduine project.....	12
Table 4-1: Manning's roughness coefficient of smooth concrete.....	15
Table 4-2: Manning's roughness coefficients of plane wood, unfinished concrete and masonry cemented rubble .....	16
Table 4-3: Manning's roughness coefficients of sand .....	17
Table 5-1: Overtopping test parameters for selected cases (1/25 model scale) .....	18
Table 5-2: Comparison of wave transformation (n=0.000 vs n=0.012).....	21
Table 5-3: Bi-chromatic wave test cases (11 Cases) .....	23
Table 5-4: Test conditions for Case 1A-1C.....	30

## List of figures

Figure 3-1: Sketch of the physical flume as in SCANDURA.....	5
Figure 3-2: Scheme of the instruments along the beach in SUSCO .....	6
Figure 3-3: CIEM configuration for the WISE Benchmark experiments with the initial profile .....	7
Figure 3-4: Layout of the ICODEP engineered beach and instruments.....	8
Figure 3-5: Model geometry WaLoWa .....	10
Figure 3-6: Experimental set-up of the CHEN project .....	11
Figure 3-7: Physical and numerical model domains for Wenduine physical model test. ....	12
Figure 4-1: Surface texture of unfinished concrete (left) and masonry cemented rubble (right) .....	17
Figure 5-1: Comparison of wave overtopping discharge with different Manning's roughness coefficient (Wenduine case).....	19
Figure 5-2: Comparison of wave overtopping discharge with different Manning's roughness coefficient (Chen's case).....	21
Figure 5-3: Physical model settings (top) and SWASH result (below) .....	22
Figure 5-4: Wave gauge numbering in SWASH .....	24
Figure 5-5: Comparison of time series in Bi_01_4 case (SWASH vs Physical model) .....	25
Figure 5-6: Comparison of time series in Bi_02_6_R case (SWASH vs Physical model).....	25
Figure 5-7: Quality of time transformation from WG1 to WG3 between 'good' case (upper 3 panels) and 'excellent' case (lower 3 panels) and WG7s.....	26
Figure 5-8: WG position on the dike in SWASH.....	27
Figure 5-9: Comparison of time series of eta and force in Bi_02_6_R case (SWASH vs Physical model) .....	27
Figure 5-10: Comparison of wave transformation and force estimation with different bottom friction parameters. ....	28
Figure 5-11: Example of numerical model bottom setting in Pax&Cox's study .....	29
Figure 5-12: Wave run-up criteria (i.e. minimum water level).....	30
Figure 5-13: Output example of wave run-up time series (blue) and smoothed one (red).....	31
Figure 5-14: Output example of spectrum at three wave gauge locations and entire and part of wave run-up time series .....	31
Figure 5-15: SWASH wave run-up result vs Stockdon model ( $n=0.019$ ) .....	32
Figure 5-16: Comparison of normalized wave run-up between SWASH and empirical models.....	33
Figure 5-17: Estimation of wave run-up conducted by Fiedler et al. (2018).....	34

# 1 Introduction

The wave overtopping calculation method for the Safety assessment 2015 was defined in Suzuki et al. (2016). In this methodology, it is stipulated that the numerical model SWASH (Zijlema et al., 2011b) and an empirical equation (Altomare et al., 2016) need to be used for wave overtopping calculation. SWASH is a process-based numerical wave model, capable of calculating a series of wave overtopping events during a storm. Therefore, it has more applicability compared to an empirical equation, which gives only an average wave overtopping estimate based on physical model tests results (using simplified geometries), for estimation of wave overtopping over a realistic configuration such as a dike with a vertical storm wall on its crest (Suzuki et al., 2017a).

Even though SWASH is a process-based model, not all physical processes are included in the methodology for wave overtopping calculation, partly on purpose. One example is the exclusion of bottom friction. In order to get a more conservative overtopping value for the safety assessment, the Manning's roughness coefficient  $n$  in the SWASH 1D overtopping calculation was deliberately set as zero. This choice however impacts the estimation of wave overtopping over a cross shore profile which includes a foreshore having a 'dry beach' part in front of the dike. Normally, a sandy beach should add dissipation to wave propagation because of its roughness. Being excluded in the aforementioned methodology, this leads to an overestimation of wave overtopping. Note that infiltration which might influence to the overtopping discharge is not dealt in this report.

In this study, the bottom friction parameter in SWASH is further explored for overtopping calculation under a condition with long berm (e.g. 50 m) in front of the dike.

The methodology of this study is as follows. First, a literature review on the relevant study is conducted in Chapter 2. One of the purpose of the literature review is to find material to study on the bottom friction effect. Second, available data is explored in order to find extra material to study in Chapter 3. Next, an overview is presented of the SWASH model and Manning's bottom friction parameters in open-channel flow in different materials. This Chapter 4 also includes a relevant discussion on the scale and possible ranges of Manning's coefficient values representing the roughness of sand and a dike promenade. After that, the SWASH model is used to study bottom friction effect (mainly by sensitivity analysis), including some extra validation of SWASH in Chapter 5. Finally some conclusions are drawn from this study in Chapter 6.

## 2 Literature review

The purpose of this study is to investigate Manning's bottom friction parameter for wave overtopping calculation in SWASH under a berm condition (i.e. long sandy beach in front of the dike). Even though the ultimate target is to estimate accurate overtopping discharge, a study on wave run-up is also relevant for this study since the main concern is the behavior of wave or bore running up on sand. Therefore the literature review is specially focused on wave run-up. Note that the literature review on Manning coefficient and relevant studies, and also SWASH, are conducted in Chapter 4.

In general, overtopping occurs when maximum wave run-up exceeds the crest of dune or structure. Therefore run-up is of great importance for coastal protection and many research has been done by the Coastal Engineering community. Due to its complex feature (e.g. the interaction of run-up and run-down) mostly the relationship between wave parameters and run-up is expressed by empirical equations, similar as for wave overtopping.

One of the popular methods is to relate wave run-up with the Iribarren number (in other words: surf-similarity parameter). The Iribarren number is expressed as

$$\varepsilon = \frac{\tan\beta}{\sqrt{H/L}} \quad (1)$$

where  $\beta$  is the characteristic slope angle,  $H$  is wave height and  $L$  is wave length.

Holman (1986) developed empirical wave run-up model using this expression based on field measurement conducted at Duck, NC, USA. The equation is expressed as follows.

$$\frac{R_{2\%}}{H_0} = 0.83\varepsilon + 0.2 \quad (2)$$

where  $R_{2\%}$  is the run-up value exceeded by 2% of the run-up events and  $H_0$  is significant wave height.

Mase (1989) also developed a similar run-up equation based on the physical model test in a wave flume with plane slopes ranging from 1/30 to 1/5. The equation is as follows.

$$\frac{R_{2\%}}{H_0} = 1.86\varepsilon^{0.71} \quad (3)$$

More recently Stockdon et al. (2006) developed another wave run-up model as below.

$$R_{2\%} = 1.1 \left( 0.35 \tan\beta \sqrt{H_0 L_0} + 0.5 \sqrt{H_0 L_0 (0.563 \tan\beta^2 + 0.0004)} \right) \quad (4)$$

In addition to those studies, a number of equations are proposed in literature, such as van der Meer & Stam (1993), De Waal and Van der Meer (1992) and Vandermeer (1998). Those are summarized in e.g. EurOtop II manual (Allsop *et al.*, 2016).

Apart from articles dealing with the empirical equations, some numerical studies on wave run-up are also found in literature. Those are more relevant to this study since the final purpose of this study is to find appropriate bottom parameter to be used in the numerical model, SWASH.

From those numerical studies, Park & Cox (2016) is particularly interesting for this study since it investigates wave run-up on a long berm. Empirical equations were developed based on their numerical model (Boussinesq equation based model) which has been validated with field measurement. Tested cases have similar dry beach length as can be found in Belgian coast after beach nourishment (cfr Knokke beach nourishment). This case will be further explored using SWASH in this study. The study result is shown in Chapter 5.

Fiedler *et al.* (2018) is also a very relevant article to this study since they used the SWASH model and have proven that SWASH can be applicable to wave run-up estimation on steep and mildly sloping natural

beaches. In the end they suggested to use  $n=0.019$  as Manning bottom friction parameter for the estimation of wave run-up in the natural beach. This study provides an interesting scope but some important discussion about directional spreading effect is still missing. The detailed discussion is found in the last chapter of this report.

## 3 Data screening

### 3.1 Description of available datasets

Seven different datasets have been identified (Table 3-1) as potential datasets for the calibration of bottom friction in SWASH. Most of the campaigns have been carried out in large-scale facilities. Five of them have used mobile bed, meanwhile two are characterised by fixed bottom over the whole length of the wave facility. Three of seven datasets refer to experimental campaign carried out in the large-scale wave flume CIEM at Universitat Politècnica de Catalunya (UPC) in Barcelona, Spain. One experimental campaign has been carried out in the Grosser Wellenkanal (GWK) in Hannover, Germany and one in the new Delta Flume at Deltares, in The Netherlands, these are one of the largest wave facilities worldwide. The last two datasets come from physical model tests carried out at Flanders Hydraulics Research (FHR). Chen's dataset was developed in a STW-programme on integral and sustainable design of multifunctional flood defences, Project No. 12760. The Wenduine test case was carried out in FHR for the design of new storm wall in Wenduine. The name and facility of each dataset are listed hereafter:

Table 3-1: Available dataset for the calibration of bottom friction in SWASH

Project name (facility)	Facility size	Mobile/fixed bed
SCANDURA (UPC)	Large	Mobile
SUSCO (UPC)	Large	Mobile
WISE (UPC)	Large	Mobile
ICODEP (GWK)	Large	Mobile
WALOWA (Deltares)	Large	Mobile
CHEN (FHR)	Non-large	Fixed
WENDUINE (FHR)	Non-large	Fixed

#### SCANDURA

The SCANDURA project aimed at obtaining new data about flow velocity in a large scale wave flume where the bottom boundary layer is in the turbulent regime. The measurements provided instantaneous velocities along the vertical, offshore of the breaker line, in presence of an erodible bed and, in turn, in presence of small scale bed forms.

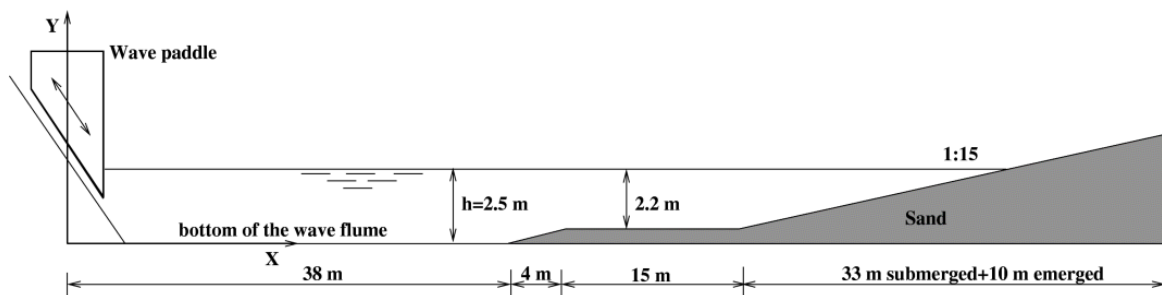
The experiments have been carried in the CIEM large wave flume at the UPC (Universitat Politècnica de Catalunya). The wave flume is 100 m long, 3 m wide and 5 m deep. A sketch is reported in Figure 3-1. The profile follows the geometry of an initial slope (0.3 m height in 4 m length), followed by a flat profile along the next 15 meters and a final second slope (1/15) 43 m long. The velocity measurements have been carried out at 4 different positions along the channel, two positions along the slope, one in the horizontal part and a last one close to the beginning of the slope. The velocities have been measured along the water depth by using an array of 8 ADVs, while close to the bottom an UVP (Ultrasonic velocimeter profiler) have

been used. The location of these instrumentation changed during the experiments in order to study the profile at different flume locations. Water surface elevation has been measured along the flume by means of resistance type wave gauges and Micro Acoustics wave-gauges (AWGs). Some of the AWGs are located in the surf zone and swash zone (between 50 and 67m from the wave paddle position at rest).

Table 3-2: Details of SCANDURA project

<b>Infrastructure</b>	CIEM
<b>Flume bottom</b>	mobile bed (sand, $d_{50}=246\mu\text{m}$ )
<b>Generated waves</b>	2 <sup>nd</sup> order monochromatic waves with AWAS

Figure 3-1: Sketch of the physical flume as in SCANDURA



## SUSCO

The SUSCO project aimed at using the Hydralab III facility at UPC to investigate shoreline response and the swash zone hydrodynamics when grouping waves, able to generate free waves and energy in the high frequency part of the spectra, impact on the controlled area.

The experiments have been carried in the CIEM large wave flume at the UPC (Universitat Politècnica de Catalunya). The types of measurements that have been performed are:

- Beach profile evolution;
- Wave characteristics;
- Run and set-up;
- Velocities inside the SZ;
- High frequency measures of longshore-crossshore sediment concentration within the SZ;
- High frequency measures of height bed bottom over the entire SZ.

The following instrument have been used during the experimental campaign:

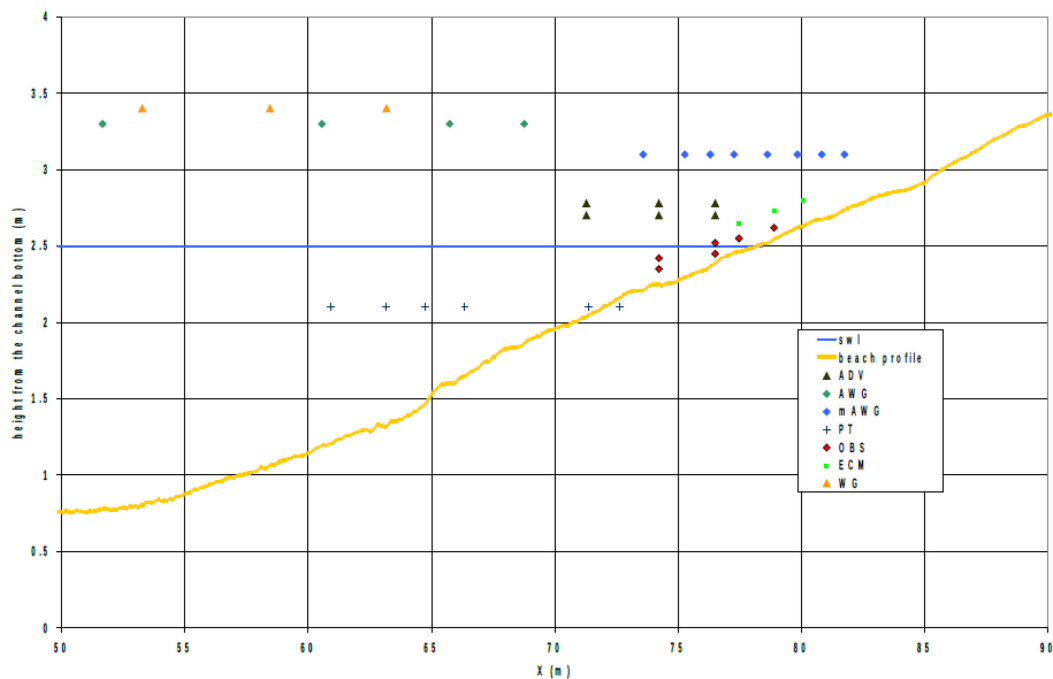
- 1 Profiler
- 6 ADVs
- 10 Resistant Wave Gauges
- 8 Micro Acoustic Wave Gauges
- 4 Acoustic Wave gauges
- 8 Optical Backscatter Sensor
- 6 Electromagnetic Current Meters
- 6 Pressure Sensors.

Location of the instruments along the beach is depicted in Figure 3-2.

Table 3-3: Details of SUSCO project

<b>Infrastructure</b>	CIEM
<b>Flume bottom</b>	mobile bed (sand, $d_{50}=246\mu\text{m}$ )
<b>Generated waves</b>	2 <sup>nd</sup> order regular monochromatic, combination of free standing long waves plus monochromatic short waves, bi-chromatic waves, random waves with AWAS

Figure 3-2: Scheme of the instruments along the beach in SUSCO



## WISE

These tests have been done in order to study the bottom evolution when reproducing 36 times the same random time series. Wave conditions are  $H_s = 0.47$  m with  $T_p = 3.7$  s following a Jonswap Spectrum with gamma 3.3 using always the same seeding number. A profile has been taken after each time series, while wave evolution, velocity and suspended sediment concentrations were measured mainly on the bar and in the swash zone.

The experiments have been carried in the CIEM large wave flume at the UPC (Universitat Politècnica de Catalunya). A sketch of the flume with location of all instruments is reported in Figure 3-3.

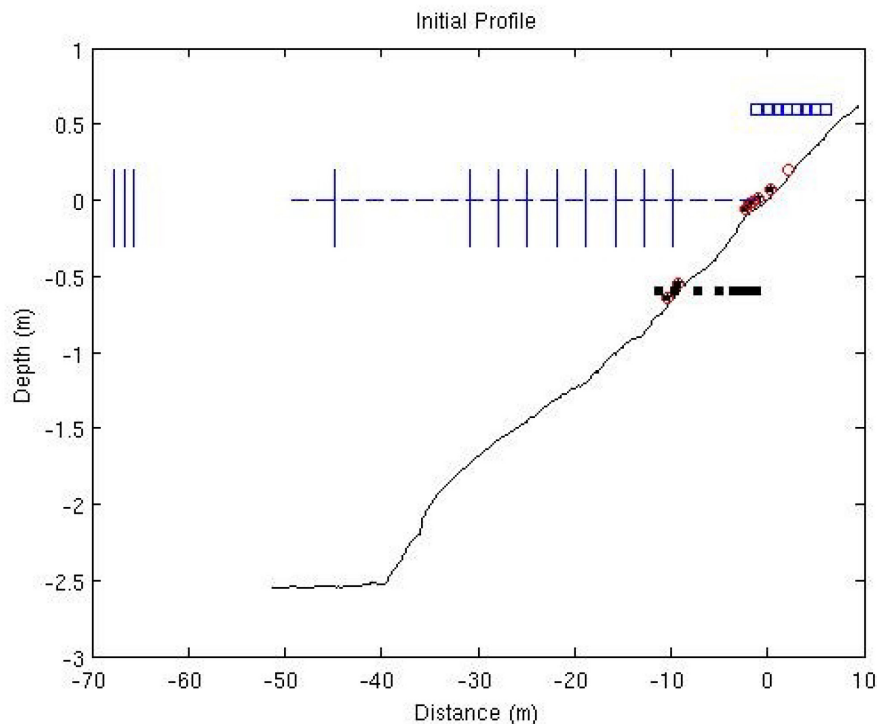
The following instrument have been used:

- ADV
- Resistance Wave Gauges
- Acoustic Wave Gauges (medium range)
- Profiler
- Optical Backscatter Sensor (OBS)
- Pressure Sensors.

Table 3-4: Details of WISE project

<b>Infrastructure</b>	CIEM
<b>Flume bottom</b>	mobile bed (sand, $d_{50}=246\mu\text{m}$ )
<b>Generated waves</b>	2 <sup>nd</sup> order random waves with AWAS

Figure 3-3: CIEM configuration for the WISE Benchmark experiments with the initial profile (solid black line). The marks show the position for Resistive Wave Gauges (solid blue lines), ADVs (solid black pentagram), OBSs (empty red circles), PPT (solid black squares) and AWGs (empty blue squares).



## ICODEP

The experimental investigation focuses on the analysis of the influence of bed mobility on wave overtopping and wave loads on a flood defense structure. A large-scale model of a sloped seawall and a foreshore is set up in a wave flume. The incoming wave and mean water level conditions are chosen in order to be representative of a typical storm in a macro tidal regime.

The experimental set-up consists of a 10/1 sloped steel seawall and a natural sandy foreshore with an initial 1/15 steepness. The sand available at the GWK was used with nominal diameter ( $d_{50}$ ) of 0.30 mm. A layout of the experimental set up is shown in Figure 3-4.

The measured parameters are listed as follows:

- Incident and reflected wave measured by means of Resistance Wave Gauges (WG) and Acoustic Wave Gauges (US).
- Morphodynamics of the sandy beach, through: measurements of the beach profiles by means of a mechanical profiler and of the 3D laser scanner, measurements of the velocity field and the sediment concentration along the beach (ADV, ABS). Information on the beach saturation condition

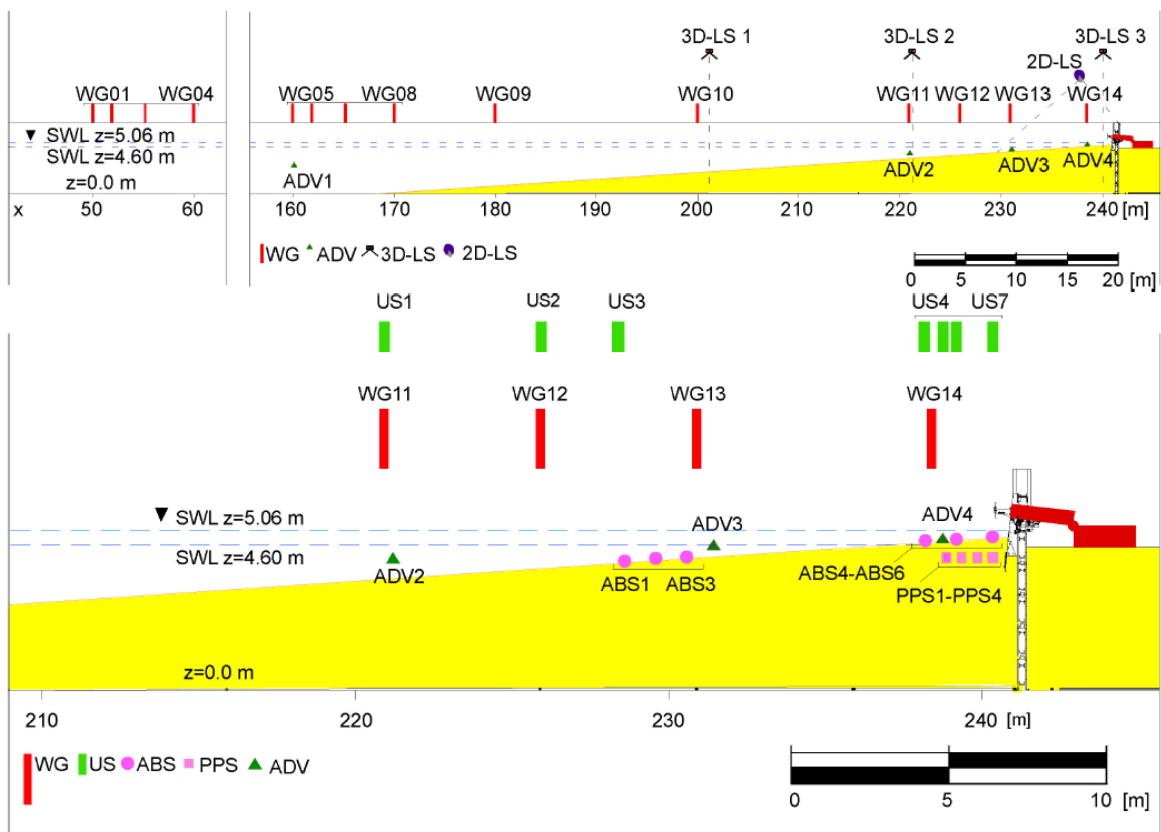
are also acquired by the pore pressure sensors (PPS) located on the sand in front of the structure below the toe level.

- Morphology of the scour at the toe of the structure with laser scanner (3D and s2D).
- Impacts on the structures are measured with pore pressure transducers (PS) and load cells.
- Overtopping volume, from the analysis of the load cells located below the overtopping tank coupled with measurement of the pumping function and time operation.

Table 3-5: Details of ICODEP project

<b>Infrastructure</b>	Grosser Wellenkanal (GWK)
<b>Flume bottom</b>	mobile bed (sand, $d_{50}=300\mu\text{m}$ ) and a steel wall
<b>Generated waves</b>	2 <sup>nd</sup> order random waves with AWAS

Figure 3-4: Layout of the ICODEP engineered beach and instruments. Upper panel: overview of the flume. Lower panel: close up on the structure.



## WALOWA

WALOWA aimed at studying the overtopped wave loads on walls in shallow foreshore conditions with particular focus on the impact mechanism and on the scale effects, by comparing the results from small

scale tests (1/25) with those obtained in the Delta Flume (model scale 1/4.3). The study of the scale effect is now on-going, so the report on this item has not been available yet.

The experiments were carried out in the new Delta Flume at Deltares, in Delft (The Netherlands). A sketch of the flume with wave gauge location is depicted in Figure 3-5. A foreshore of compacted sand was constructed within the Delta Flume. The  $d_{50}$  was  $320\mu\text{m}$ . This sand was only installed for the 0.4m top layer over the entire foreshore. Below the 0.4 m top layer was a sand with  $d_{50} = 230\mu\text{m}$  installed. The erosion depth over the entire foreshore never exceeded 0.4m during the tests. The foreshore starts at location  $X = 93.98$  m from the paddle and is comprised of a transition slope (1/10) until 1.95 m flume height and attached a beach slope (1/35) until 3.71 m flume height. The end of the foreshore is the dike toe location  $X = 175.08$  m from the paddle. Connected to the foreshore is a 0.53 m high dike structure with a 1/2 slope. On the dike a 2.32m wide promenade is built and at the end of the promenade a non-overtopped wall of 1.6 m height is constructed. The promenade has a 1/100 seaward slope to facilitate drainage of water.

The following instrument were used during the experimental campaign:

- WaveGuide wave radar
- 7 Resistance Wave Gauges (WHM) along the wave flume
- Kulite HKM-379 (M) pressure sensors
- HBM U9 load cells
- Wave gauges on promenade
- MaxSonar HRXL/ Honeywell 943 M18 ultrasonic distance sensors
- Valeport 802 electro-magnetic current meter
- Airmar flow meter S300 paddle wheels
- High speed camera
- Void-fraction meter
- SICK LMS511 laser profiler
- ASM-IV-N argus surface meter
- Mechanical profiler

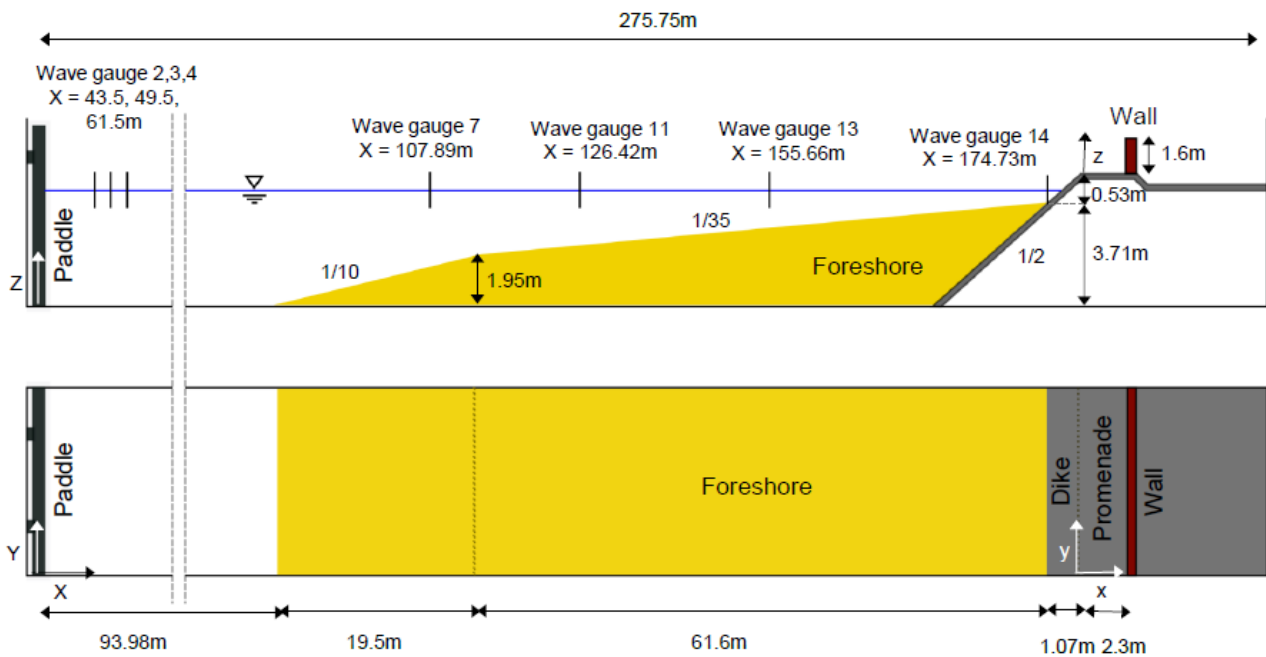
Using the above listed measurements, the following parameters were measured during the campaign:

- water surface elevation
- sand concentration
- bottom profile
- layer thickness on the promenade
- layer velocity on the promenade
- impact forces on wall
- impact pressure on wall
- void-fraction in front of the wall
- High speed camera recording from behind wall
- Laser profile of dike, promenade and wall
- Video recordings from top, side and behind wall

Table 3-6: Details of WALOWA project

<b>Infrastructure</b>	New Delta Flume
<b>Flume bottom</b>	mobile bed (sand, $d_{50}=320\mu\text{m}$ for the foreshore 40cm-top-layer and $d_{50}=230\mu\text{m}$ for the foreshore bottom layer) with concrete dike after the foreshore
<b>Generated waves</b>	1 <sup>st</sup> and 2 <sup>nd</sup> order random and bichromatic waves with AWAS

Figure 3-5: Model geometry WaLoWa



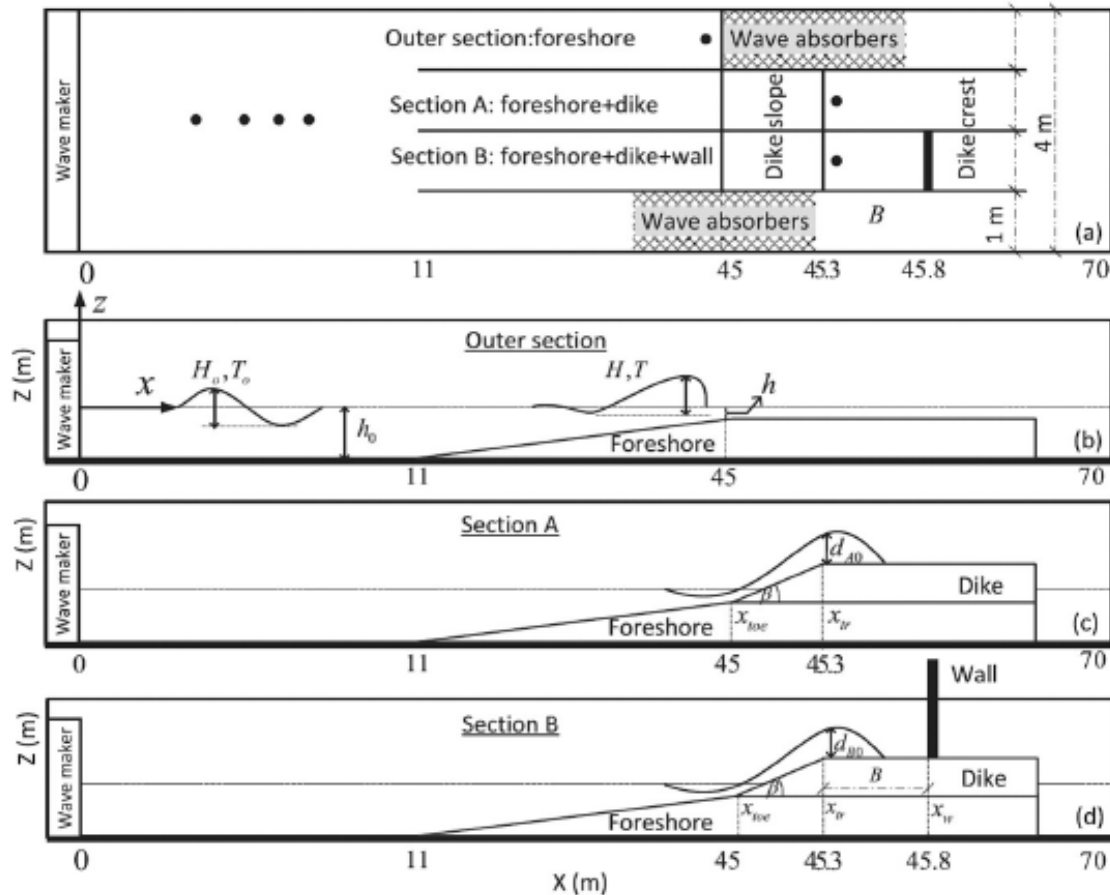
**CHEN**

Physical model tests were performed in a 4 m wide, 1.4m deep and 70 m long wave flume at Flanders Hydraulic Research, Antwerp, Belgium. A piston-type wave generator with a stroke length of 0.6 m was used generating monochromatic, bi-chromatic and random waves, but without an active wave absorption system. The wave flume was split into four sections (1 m for each), as shown in in Figure 3-6. The wave overtopping was measured in section A meanwhile the incident wave boundary conditions were measured in the outer section. Section A was used to measure the unobstructed overtopping flow features along the dike crest and Section B was used to measure the impact force of overtopping flows. Layer thickness on the sea dike was measured by means of 6 resistive wave gauges, 3 in Section A and 3 in Section B. To characterize the velocity field close to the wall, video camera recording together with Bubble Image Veociometry was implemented.

Table 3-7: Details of CHEN project

<b>Infrastructure</b>	Large wave flume at FHR
<b>Flume bottom</b>	fixed concrete bottom and a wooden dike
<b>Generated waves</b>	1 <sup>st</sup> order regular monochromatic, bi-chromatic waves, random waves without AWAS

Figure 3-6: Experimental set-up of the CHEN project



## WENDUINE

The purpose of the study is to provide necessary information for the design of storm wall in Wenduine. Tests were performed at 1/25 scale in the large wave flume at Flanders Hydraulics Research (Antwerp, Belgium). The flume is 70 m long, 1.5 m high and 4 m wide. A piston-type wave generator with a stroke of 0.5 m was used for wave generation with a passive wave absorption system located downstream of the sea-dike. The maximum water depth at the wave generator is 1.2 m. For physical model tests a JONSWAP wave spectrum with  $\gamma = 3.3$  was generated with the wave paddle and the total number of waves generated was about 1000. Wave height measurements were obtained with twelve resistance type wave gauges installed at the locations summarized in Figure 3-7. Mean wave overtopping discharge was obtained by dividing the total volume of water collected in an overtopping box during a test by the total duration of the test.

A limitation in this experimental campaign is the use of first-order wave generation and the lack of active wave absorption. However, as proven in Altomare et al. (2016), the influence of the lack of active wave absorption is negligible. Also, the influence of cross waves was also found to be negligible as detailed in Altomare et al. (2016). Note that incident time series estimated from three offshore wave gauges were used in the validations, therefore the first-order wave generation and lack of active wave absorption are not really limitations for those validation cases.

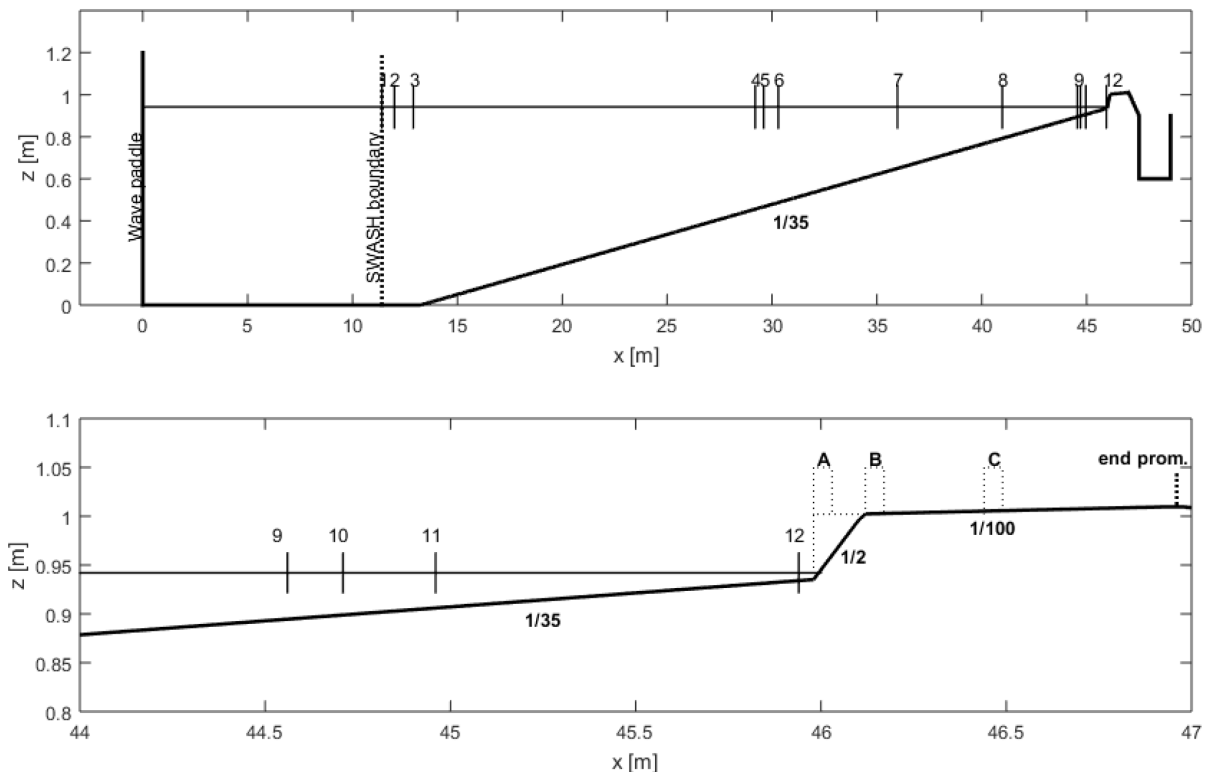
As can be seen in Figure 3-7, storm walls are positioned at different location on the dike: 'A' configuration denotes a vertical dike plus a vertical wall immediately behind the 1/35 shallow foreshore slope; 'B' configuration is a 1/2 sloping dike and a vertical wall at the end of the dike slope; and 'C' configuration is a vertical wall in the middle of the dike. The vertical wall was omitted in three test cases (refer as

“WEN\_004”, “WEN\_024” and “WEN\_026”). The mean overtopping discharge for these test cases cannot be estimated by existing semi-empirical equations due to the relatively complex configuration of a promenade combined with a storm wall in a very shallow foreshore. Note that if this were a deep water condition, the equation of (Van Doorslaer et al., 2015) could be used to estimate mean wave overtopping discharge, or if the storm wall was not present on the dike the empirical equation introduced by Altomare et al. (2016) would be applicable.

Table 3-8: Details of Wenduine project

<b>Infrastructure</b>	Large wave flume at FHR
<b>Flume bottom</b>	fixed bottom with wooden dike
<b>Generated waves</b>	1 <sup>st</sup> order irregular waves without AWAS

Figure 3-7: Physical and numerical model domains for Wenduine physical model test.  
 Upper panel shows the entire model domain including location of wave gauges 1 to 12.  
 Lower panel shows close up of sea dike and sea wall configuration “A”, “B” and “C” with dashed lines.



## 3.2 Discussions and conclusions

Most of the experimental test campaigns (i.e. SCANDURA, SUSCO, WISE, ICODEP, WALOWA) used sand as bottom and therefore there were changes in bathymetry during one test. On top of that, none of them has a long and dry berm in those tests. Therefore those would be difficult to be used for the validation/tuning a fixed bed model SWASH for overtopping over sand berms. On the other hand, FHR and the associated research group have conducted preliminary SWASH calculations and good scopes how to use SWASH are available for ICODEP and WALOWA cases even though they used mobile bed. Data from WALOWA will be most useful since some test cases were using bi-chromatic waves (i.e. short duration test) and thus the bathymetry change during the tests is limited. Even though the berm effect cannot be fully discussed, we decided to use WALOWA tests for the further investigation of SWASH settings. The ICODEP case is also used to see the behaviour of SWASH.

Apart from those cases, the CHEN and WENDUNE test will also be used since FHR has a good knowledge of those physical models (Altomare et al., 2016) and also SWASH modelling (Suzuki et al, 2017b) for those datasets.

All relevant calculation and results are shown in Chapter 5.

## 4 Model

### 4.1 SWASH model

SWASH is an open source deterministic time domain wave model. The governing equations of the model are the non-linear shallow water equations with added non-hydrostatic effects. The one-dimensional, depth-averaged shallow water equations in non-conservative form are shown as follows:

$$\frac{\partial \zeta}{\partial t} + \frac{\partial hu}{\partial x} = 0 \quad (5)$$

$$\frac{\partial u}{\partial t} + u \frac{\partial u}{\partial x} + g \frac{\partial \zeta}{\partial x} + \frac{1}{2} \frac{\partial p_b}{\partial x} + \frac{1}{2} \frac{p_b}{h} \frac{\partial(\zeta - d)}{\partial x} + c_f \frac{u|u|}{h} = 0 \quad (6)$$

$$\frac{\partial w_s}{\partial t} = \frac{2p_b}{h} - \frac{\partial w_b}{\partial t}, w_b = -u \frac{\partial d}{\partial x} \quad (7)$$

$$\frac{\partial u}{\partial x} + \frac{w_s - w_b}{h} = 0 \quad (8)$$

where  $t$  is time,  $x$  the horizontal coordinate,  $u$  the depth averaged velocity in  $x$ -direction,  $w_s$  and  $w_b$  the velocity in  $z$ -direction at the free surface and at the bottom, respectively.  $\zeta$  is the free-surface elevation from still water level,  $d$  is the still water depth and  $h$  the total depth.  $p_b$  is the non-hydrostatic pressure at the bottom,  $g$  the gravitational acceleration and  $c_f$  the dimensionless bottom friction coefficient.

The bottom friction coefficient  $c_f$  is expressed by Manning's roughness coefficient  $n$  as follows:

$$c_f = \frac{n^2 g}{h^{1/3}} \quad (9)$$

Note that Manning coefficient  $n$  is a dimensional parameter [ $s/m^{1/3}$ ].

Eqs. (5) and (8) are the global and local continuity equations, respectively, to assure both local and global mass conservation. Eq. (6) is the momentum equation for the  $u$ -velocity which includes the effect of non-hydrostatic pressure and bottom friction. Note that momentum conservation is obtained at the discrete level in line with (Stelling & Duinmeijer, 2003). First equation of Eq. (7) is the momentum equation for the vertical velocity at free surface  $w_s$ . The vertical velocity at the bottom  $w_b$  is described by means of the kinematic condition as presented by the last part of Eq. (7).

Note that the governing equations are based on the incompressible Navier-Stokes equations when multiple layers in the vertical are considered. In this way we take into account the vertical structure of the horizontal flow. In this study all calculations have been conducted in one single layer, i.e. depth-averaged, which appeared to be sufficient with respect to frequency dispersion related to wave transformation and suitable for wave overtopping calculation in terms of computational stability.

A full description of the numerical model based on a staggered, conservative, finite-difference scheme, different kinds of boundary conditions, and different types of applications are given in Rijnsdorp & Zijlema (2016), Smit et al. (2013) and Zijlema et al. (2011).

## 4.2 Bottom friction approaches in SWASH

In the user manual of SWASH describes the bottom friction approaches in SWASH as follows:

*For typical depth-averaged calculations, four different bottom friction values are available, i.e., constant, Chezy, Manning and Colebrook-White values. Note that the Colebrook-White friction value equals the Nikuradse roughness height. Although they are associated with depth-averaged flow velocities, they may be applied in the multi-layered mode as well. However, some inaccuracies may occur in the vertical structure of the velocity, in particular when the depth-averaged velocity is zero. Alternatively, the logarithmic wall law may be applied. In this case, a distinction is made between smooth and rough beds. For rough beds, the user must apply a Nikuradse roughness height. The aforementioned friction formulations are usually derived for quasi-steady flow condition (e.g. flow in a river). However, numerical experiments have indicated that the Manning formula provides a good representation of wave dynamics in the surf zone, and even better to that returned by other friction formulations.*

In this study we only applied Manning approach to include bottom friction effect in line with Suzuki et al. (2017b) and Zijlema et al. (2011). The reasoning to choose the Manning approach is that this expression provides a better representation of wave dynamics in the surf zone to that returned by other well-known friction formulations such as the one in terms of the Chézy coefficient and the Colebrook–White equation, according to Zijlema *et al.* (2011). As described above, Manning bottom friction approach can be applied to multi-layered mode as well. The applicability and results will be shown in Chapter 5.

## 4.3 Manning approach

### 4.3.1 Manning coefficient

The Manning formula is developed by R. Manning in 1891 which characterizes the flow in channels. According to that theory flow velocity characteristics of open channels are dependent on the slope of the bed, the roughness of the channel, and the hydraulic radius of the channel. The empirical value of the Manning coefficient has been studied for long time and we can access to those in literature. Some examples are shown below.

Note that application of those values are discussed in the next section.

Table 4-1: Manning's roughness coefficient of smooth concrete

Streambed Characteristics	Roughness Coefficient
Mountain streams with rocky beds	0.04-0.05
Winding natural streams with weeds	0.035
Natural streams with little vegetation	0.025
Straight, unlined earth canals	0.020
Smoothed concrete	0.012

Source: <https://serc.carleton.edu/details/images/9159.html>

Table 4-2: Manning's roughness coefficients of plane wood, unfinished concrete and masonry cemented rubble

## Manning's n for Channels (Chow, 1959).

Type of Channel and Description	Minimum	Normal	Maximum
<b>5. Lined or Constructed Channels</b>			
<b>a. Cement</b>			
1. neat surface	0.010	0.011	0.013
2. mortar	0.011	0.013	0.015
<b>b. Wood</b>			
1. planed, untreated	0.010	0.012	0.014
2. planed, creosoted	0.011	0.012	0.015
3. unplanned	0.011	0.013	0.015
4. plank with battens	0.012	0.015	0.018
5. lined with roofing paper	0.010	0.014	0.017
<b>c. Concrete</b>			
1. trowel finish	0.011	0.013	0.015
2. float finish	0.013	0.015	0.016
3. finished, with gravel on bottom	0.015	0.017	0.020
4. unfinished	0.014	0.017	0.020
5. gunite, good section	0.016	0.019	0.023
6. gunite, wavy section	0.018	0.022	0.025
7. on good excavated rock	0.017	0.020	
8. on irregular excavated rock	0.022	0.027	
<b>d. Concrete bottom float finish with sides of:</b>			
1. dressed stone in mortar	0.015	0.017	0.020
2. random stone in mortar	0.017	0.020	0.024
3. cement rubble masonry, plastered	0.016	0.020	0.024
4. cement rubble masonry	0.020	0.025	0.030
5. dry rubble or riprap	0.020	0.030	0.035
<b>e. Gravel bottom with sides of:</b>			
1. formed concrete	0.017	0.020	0.025
2. random stone mortar	0.020	0.023	0.026
3. dry rubble or riprap	0.023	0.033	0.036
<b>f. Brick</b>			
1. glazed	0.011	0.013	0.015
2. in cement mortar	0.012	0.015	0.018
<b>g. Masonry</b>			
1. cemented rubble	0.017	0.025	0.030
2. dry rubble	0.023	0.032	0.035
<b>h. Dressed ashlar/stone paving</b>	0.013	0.015	0.017
<b>i. Asphalt</b>			
1. smooth	0.013	0.013	
2. rough	0.016	0.016	
<b>j. Vegetal lining</b>	0.030		0.500

Source: [http://www.fsl.orst.edu/geowater/FX3/help/8\\_Hydraulic\\_Reference/Mannings\\_n\\_Tables.htm](http://www.fsl.orst.edu/geowater/FX3/help/8_Hydraulic_Reference/Mannings_n_Tables.htm)

Table 4-3: Manning’s roughness coefficients of sand

Table 1. Base Values of Manning's <i>n</i>			
Bed Material	Median Size of bed material (in millimeters)	Base <i>n</i> Value	
		Straight Uniform Channel <sup>1</sup>	Smooth Channel <sup>2</sup>
<b>Sand Channels</b>			
Sand <sup>3</sup>	0.2	0.012	--
	.3	.017	--
	.4	.020	--
	.5	.022	--
	.6	.023	--
	.8	.025	--
	1.0	.026	--
<b>Stable Channels and Flood Plains</b>			
Concrete	--	0.012-0.018	0.011
Rock Cut	--	--	.025
Firm Soil	--	0.025-0.032	.020
Coarse Sand	1-2	0.026-0.035	--
Fine Gravel	--	--	.024
Gravel	2-64	0.028-0.035	--
Coarse Gravel	--	--	.026
Cobble	64-256	0.030-0.050	--
Boulder	>256	0.040-0.070	--

[Modified from Aldridge & Garret, 1973, Table 1 --No data  
<sup>1</sup>Benson & Dalrymple --No data  
<sup>2</sup> For indicated material; Chow( 1959)  
<sup>3</sup> Only For Upper regime flow where grain roughness is predominant

Source: <http://www.engr.colostate.edu/~bbledsoe/CIVE413/Arcrement&Schneider.pdf>

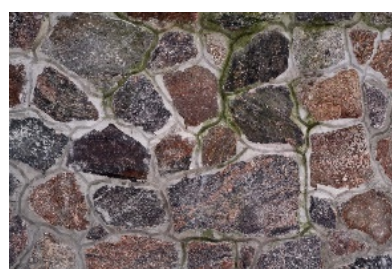
### 4.3.2 Scaling

As noticed before, the Manning roughness coefficient is a dimensional parameter (unit is [s/m<sup>1/3</sup>]). Thus scaling factor can be applied if one follows the Froude scaling law. If one follows this, scaling up from 1/25 model scale (smooth wood for dike and concrete for foreshore bottom: both n=0.012 according to Table 4-1 and Table 4-2) to prototype scale is shown below.

1/25 scale	1/1 scale
dike length 1 [m]	dike length 25 [m] (factor 25)
time 2.4 [s]	time 12 [s] (factor 25 <sup>1/2</sup> )
n=0.012 [s/m <sup>1/3</sup> ] (mainly used in SWASH)	n=0.0205 [s/m <sup>1/3</sup> ] (factor 25 <sup>1/6</sup> )

It is worth to mention that using smooth wood and concrete in 1/25 scale (n=0.012) was more or less a good representation of sand and promenade in prototype (n=0.0205): sand’s n is around 0.017 assuming that the d50 is 0.3mm and promenade’s n can be 0.017-0.025 assuming that the material on the promenade is more rough than unfinished concrete and less rough than masonry cemented rubble, see surface material below.

Figure 4-1: Surface texture of unfinished concrete (left) and masonry cemented rubble (right)



## 5 In-depth analysis of bottom friction settings in SWASH

In order to have a comprehensive overview of parameter settings of SWASH for overtopping calculation, different parameters/methods are explored here while main focus stays on bottom friction parameter, Manning roughness coefficient  $n$ .

### 5.1 Wenduine

The physical model test data of Wenduine are used for sensitivity analysis of bottom friction parameter in the SWASH model. These tests feature a smooth, impermeable sea dike (made of wood in the physical model) setup on a concrete foreshore with a constant 1/35 slope.

#### 5.1.1 Test cases

In total, eleven physical model tests, as listed in Table 5-1, were simulated with the SWASH model, where  $H_{m0}$ ,  $T_p$  are the offshore measured wave parameters at wave gauge 6 (refer to Figure 3-7). The still water levels (SWL) are measured values in the flume before the physical model test began. In these tests the SWL, wave conditions, foreshore level at the toe of the dike, wall heights and dike slopes are varied. Vertical wall elements on top of the dike, at the locations denoted 'A', 'B' and 'C', were also tested.

Table 5-1: Overtopping test parameters for selected cases (1/25 model scale)

TEST NAME	SWL	Offshore $H_{m0}$	Offshore $T_p$	DIKE SLOPE	DIKE TOE LEVEL	DIKE CREST LEVEL*	CREST LEVEL	WALL CONFIGURATION
[-]	[m]	[m]	[s]	[-]	[m]	[m]	[m]	[-]
WEN_004	0.942	0.189	2.16	1/2	0.9352	1.0024	1.0096	No wall (Dike + Prom.)
WEN_017	0.989	0.186	2.19	1/2	0.9352	1.0024	1.0504	B
WEN_018	0.989	0.185	2.19	1/2	0.9352	1.0024	1.0504	C
WEN_024	0.967	0.187	2.19	1/2	0.9352	1.0024	1.0676	No wall (only dike)
WEN_026	0.952	0.198	2.63	1/2	0.9352	1.0024	1.0676	No wall (only dike)
WEN_027	0.943	0.196	2.63	1/2	0.9352	1.0024	1.0504	C
WEN_041	0.943	0.188	2.19	1/2	0.9352	1.0024	1.0744	C
WEN_042	0.943	0.186	2.19	1/2	0.9352	1.0024	1.0504	B
WEN_124	0.952	0.186	2.19	0	0.9352	1.0104	1.0343	A
WEN_125	0.952	0.186	2.19	0	0.9352	1.0104	1.0583	A
WEN_126	0.952	0.194	2.19	0	0.9352	1.0104	1.0823	A

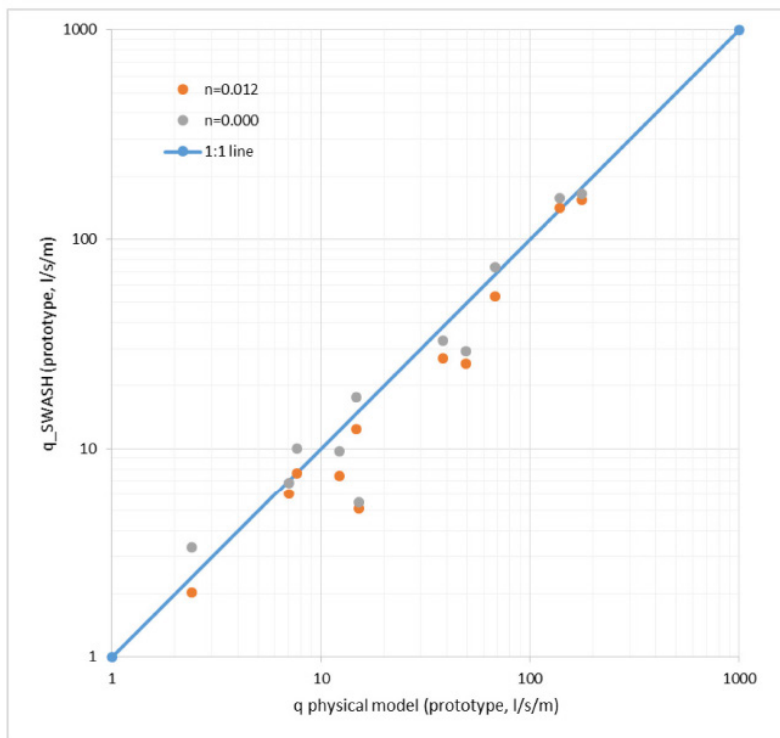
\*at the seaward edge of the dike

### 5.1.2 Results

In the safety assessment methodology book (Suzuki et al., 2016), a conservative approach, namely using bottom friction parameter  $n=0.000$  (zero-friction), has been implemented. Looking at Figure 5-1 (also in the background report Suzuki et al., 2017a) the result of  $n=0.012$  is slightly underestimating the overtopping discharge compared to  $n=0.000$ . Indeed  $n=0.000$  gives the best result in terms of the Geo parameter (The geometric mean, see equation 9). However actually both values 0.87 ( $n=0.000$ ) and 0.70 ( $n=0.012$ ) are very good value compared to other results reported in Suzuki et al. (2017a), and thus we can still concluded that  $n=0.012$  is a good parameter setting. Note that  $\text{Geo}=1$  is the perfect match.

In other words, it can be concluded that the material based  $n$  value (smooth concrete as foreshore and smooth wood as dike, both  $n=0.012$ ) gives a good result in terms of overtopping estimation using SWASH.

Figure 5-1: Comparison of wave overtopping discharge with different Manning's roughness coefficient (Wenduine case)



	Geo	GSD
$n=0.000$	0.87	1.42
$n=0.012$	0.70	1.40

Geo

$$\bar{x}_G = \exp \left[ \frac{1}{N} \sum_{i=1}^N \ln x_i \right] \text{ with } x_i = \frac{q_{est,i}}{q_{meas,i}}$$

GSD

$$\sigma(x_G) = \exp \left\{ \left[ \frac{1}{N} \sum_{i=1}^N \left( (\ln x_i)^2 - (\ln \bar{x}_G)^2 \right) \right]^{0.5} \right\}$$

## 5.2 Chen

The physical model test data of Chen are used for sensitivity analysis of bottom friction parameter in the SWASH model. These tests feature a smooth, impermeable sea dike (made of wood in the physical model) setup on a concrete foreshore with a constant 1/35 slope.

### 5.2.1 Test cases

In total, 10 physical model tests from Chen's test were simulated with the SWASH model. SWL, dike slope, dike toe level, dike crest level were fixed as 0.960 m, 1/3, 0.910 m and 1.011 m, respectively. Offshore significant wave heights were varied from 0.12 to 0.20 m and offshore peak wave period were varied from 2.0 to 2.4 s.

### 5.2.2 Results

The wave transformation and overtopping results (comparison between  $n=0.000$  and  $0.012$ ) are shown in Figure 5-2 and Table 5-2, respectively.

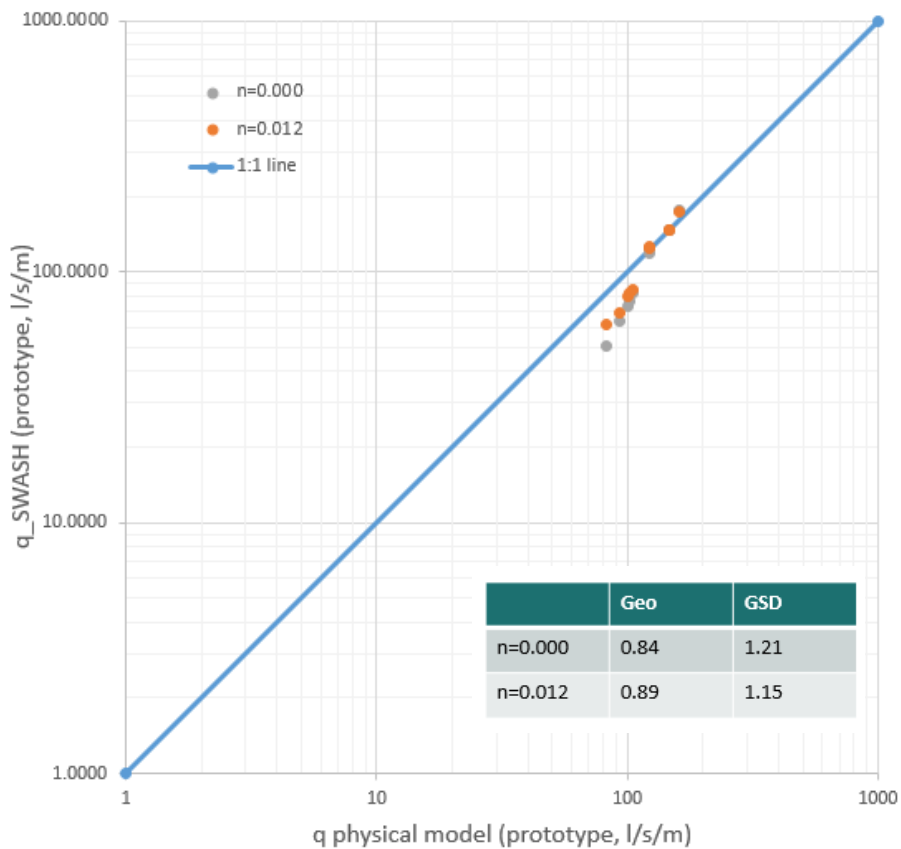
Surprisingly the result with  $n=0.000$  gives slightly lower overtopping discharge (Figure 5-2) while wave properties are almost the same (Table 5-2). The normal expectation is that the higher bottom friction case gives lower overtopping discharge. However in this case the result is opposite. This has not been well understood so far. However, again the geo values for both cases are in a very good range (in general better than ones in Wenduine) thus we can still conclude that  $n=0.012$  is a good parameter setting.

It can be concluded that the material based  $n$  value (smooth concrete as foreshore and smooth wood as dike, both  $n=0.012$ ) gives a good result in terms of overtopping estimation using SWASH.

Table 5-2: Comparison of wave transformation (n=0.000 vs n=0.012)

Case	Hm0_n0.000/n0.012	Tm-1,0_n0.000/n0.012	Set-up_differece
134	1.01	1.03	-0.001
135	1.01	1.01	-0.001
143	1.00	0.97	-0.001
144	0.99	0.94	-0.001
153	1.00	0.95	-0.002
164	1.01	1.03	0.000
174	1.02	0.99	0.000
187	1.00	0.95	0.000
189	1.02	1.03	0.000
188	1.01	0.96	0.000

Figure 5-2: Comparison of wave overtopping discharge with different Manning's roughness coefficient (Chen's case)



### 5.3 ICODEP

The physical model test data of ICODEP project are used for sensitivity analysis of bottom friction parameter in the SWASH model.

This experimental investigation focuses on the analysis of the influence of bed mobility on wave overtopping and wave loads on a flood defense structure. See details in Section 3.1.

The SWASH modelling was conducted by Giulia Mancini from Nottingham University, supervised by Dr. Ricardo Briganti. FHR also gave some advice on her SWASH modelling. Here below is from ones of her presentation ppt slide, showing the overview of the physical model.

According to her work, overtopping estimation is more accurate when the end bathymetry of each segments is used in SWASH. Note that one run is not too long (around 30 min in model scale), hence the bathymetric change within a segment is not comparable to e.g. the runs carried out for the safety assessment (45 hours in prototype).

Figure 5-3 shows the sensitivity analysis of the bottom friction parameter for overtopping estimation. The overtopping estimation result is changed by the bottom friction setting ranging from  $n=0.010$  to  $n=0.014$  at the 10:1 sloped steel wall. From this analysis  $n=0.014$  gives the best result.

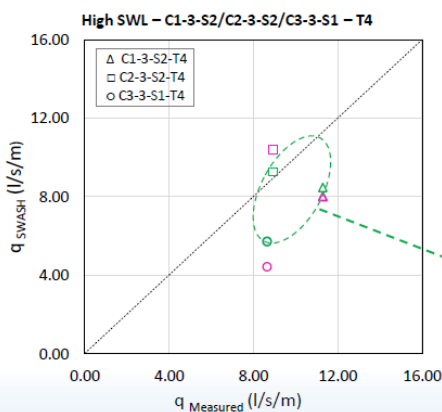
From this study also, it can be concluded that the material based  $n$  value (steel’s  $n$  would be around 0.014) gives a good result in terms of overtopping estimation using SWASH.

Figure 5-3: Physical model settings (top) and SWASH result (below)



**Experimental set-up:**

- 10:1 sloped **steel wall**
- **Wall’s crest elevation:** 5.5 m
- **Foreshore’s initial steepness:** 1:15
- **Sand:**  $d_{50} = 0.3$  mm



$$q \text{ (l/s/m)} = \frac{\int_{t_{start}}^{t_{end}} q(t) dt}{t_{end} - t_{start}}, \text{ where } q(t) = h(t) u(t),$$

$(h(t))$  and  $(u(t))$  are the water depth and overtopping velocity, respectively, extracted at the **numerical gauge** near the crest of the wall (WGOV)

Manning coefficient:	Manning coefficient:	Manning coefficient:
0.019 (sand), 0.014 (wall) $s/m^{1/3}$	0.019 (sand), 0.012 (wall) $s/m^{1/3}$	0.019 (sand), 0.010 (wall) $s/m^{1/3}$
RMSE (l/s/m)	RMSE (l/s/m)	RMSE (l/s/m)
2.18	2.69	3.20

## 5.4 WaLoWa

The physical model test data of WaLoWa project are used for further validation of SWASH (wave generation, transmission, wave transformation on the dike and force estimation) and sensitivity analysis of bottom friction parameter. These tests feature a smooth, impermeable sea dike (made of concrete in the physical model) setup on a mobile bed with initial slope of 1/35. See details in Section 3.1.

### 5.4.1 Test cases

As stated before, one of the good aspects of the WaLoWa test for the present study is that it has bichromatic wave test cases. The run time of the bichromatic wave cases are much shorter (e.g. 5 min) than one in irregular wave cases (3 hours). This data set provides an opportunity to compare wave generation, transformation, overtopping and force in a very detailed manner (i.e. irregular wave cases are typically evaluated by statistical wave parameter such as  $H_{m0}$  and  $T_{m-1,0}$ , on the other hand bichromatic wave cases can be evaluated by time series). Accordingly, possible weak points of the numerical model can be detected relatively easier.

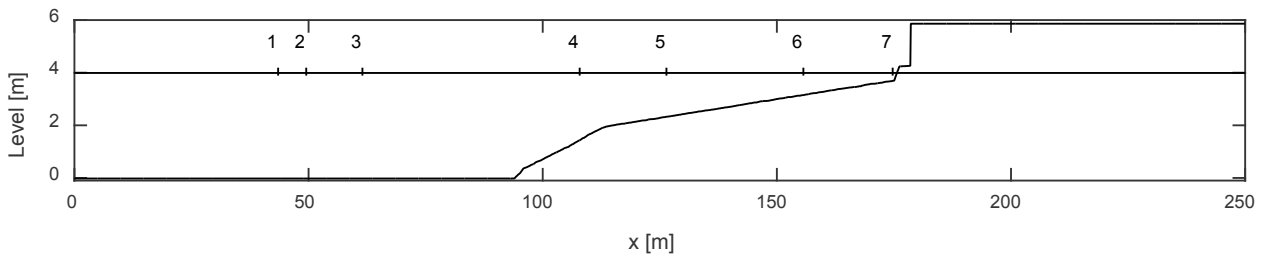
In this study, all the bichromatic wave cases (see Table 5-3) are simulated using SWASH. The input of the wave boundary condition in SWASH is the water surface elevation obtained at WG2 ( $x=43.5$  m). Note that reflection analysis was not conducted to get incident time series since the number of bichromatic waves were limited to three (reflected waves reached at WG2 right after the three bichromatic waves).

Table 5-3: Bi-chromatic wave test cases (11 Cases)

Test ID	a2/a1	f1 [Hz]	a1 [m]	omega [rad/s]	phase [°]	f2 [Hz]	a2 [m]	Omega [rad/s]	Phase [°]
Bi_01_4	1	0.174	0.5	1.0895	0	0.142	0.4	0.891	0
Bi_01_5	1	0.174	0.5	1.0895	0	0.142	0.45	0.891	0
Bi_01_6	1	0.174	0.5	1.0895	0	0.142	0.5	0.891	0
Bi_02_4	1	0.19	0.45	1.1931	0	0.155	0.36	0.976	0
Bi_02_5	1	0.19	0.45	1.1931	0	0.155	0.405	0.976	0
Bi_02_6	1	0.19	0.45	1.1931	0	0.155	0.428	0.976	0
Bi_02_6_R	1	0.19	0.45	1.1931	0	0.155	0.428	0.976	0
Bi_01_6_R	1	0.174	0.5	1.0895	0	0.142	0.5	0.891	0
Bi_03_6	1	0.1735	0.3	1.0896	0	0.142	0.3	0.891	0
Bi_03_6_1	1	0.1735	0.35	1.0896	0	0.142	0.35	0.891	0
Bi_03_6_2	1	0.1577	0.35	0.9910	0	0.129	0.35	0.811	270

The SWASH domain is modelled from  $x=43.5$  to 206.4 m in the flume. The grid size of 0.2 m is used as a standard case. The vertical wall is modelled by activating BOTCel SHIFT mode in SWASH, so that the wall is expressed correctly while the default mode without BOTCel gives one extra step in front of the vertical wall due to interpolation. As stated above, the boundary input comes from time series of water surface elevation measured at WG2. The wave boundary in SWASH is the weakly reflective boundary which theory is the same as AWAS in the wave flume. In the standard case manning bottom friction parameter  $n=0.019$  is used. The used SWASH version is always 4.01 unless otherwise stated. Wave gauges placed in the SWASH domain is 11 (7 on the flat bottom and foreshore, and 4 on the dike). The location of the seven wave gauges are depicted in Figure 5-4. To distinguish SWASH and physical model, the wave gauges in SWASH is described as e.g. 'WG7' while the physical model ones are described as e.g. 'wave gauge 14'.

Figure 5-4: Wave gauge numbering in SWASH



1-7 are represented of wave gauges placed in SWASH: WG1 –WG7 (top)

## 5.4.2 Results

### Wave generation and wave transformation

The quality of the result is roughly categorized into 2, namely ‘good’ and ‘excellent’ results in terms of wave transformation (evaluated at WG7 in SWASH, i.e. ‘wave gauge 14’ in the physical model).

One example of the ‘good’ results is shown in Figure 5-5 (case Bi\_01\_4). As can be seen the time series calculated using SWASH follow the general trend of the time series of the physical model. However, if the time series are critically evaluated, some discrepancy can be recognized e.g. WG7. The time series of WG7 is especially important since the quality of WG7 decides the quality of the estimation of the force (evaluation of the force is described later). Similar quality results are found in Bi\_01\_4, Bi\_01\_5 and Bi\_01\_6 (3 cases)

One example of the ‘excellent’ results is shown in Figure 5-6 (case Bi\_02\_6\_R). As can be seen the time series calculated using SWASH follow the trend of the time series of the physical model until toe of the dike (i.e. WG7). Similar quality results are found in Bi\_02\_4, Bi\_02\_5, Bi\_02\_6, , Bi\_01\_6\_R, , Bi\_02\_6\_R, , Bi\_03\_6, , Bi\_03\_6\_1, and Bi\_03\_6\_2 (8 cases). See all the details of the results in Appendix A. Note that the some extra oscillation found in WG7 in SWASH after the third/fourth bichromatic wave could be due to input signal. As explained earlier we used measured water surface elevation from WG1 (wave gauge 2 in physical model) and therefore it includes reflected waves. On the other hand SWASH recognized this as all incident wave and therefore SWASH generated wrong waves after reflected waves arrived at WG1. However this is not a problem since the signal after third/fourth bichromatic wave is not our interest. It could be corrected if incident wave information was given (e.g. by reflection analysis from three wave gauges). However in this study the position of the three wave gauges were not optimized for the bichromatic wave condition, so further treatment is not conducted.

Closely looking at the two different results, it can be found that the quality of time series at WG7 is decided by the quality of wave transformation close to the wave generation boundary, in other word, wave transformation from WG1 to WG3 (Figure 5-7). As can be seen in the blue circles, the wave transformation of Bi\_01\_4 is much worse than one of Bi\_02\_6\_R. This eventually resulted in less good correspondence of time series between SWASH and physical model in WG7. However the reason is not sure why the underestimation of the crest is happened. It might be due to the boundary problem: in general SWASH gives higher wave height (around 10%) at the wave boundary while this is rapidly decreased in space. However this higher wave or higher wave steepness would cause extra wave breaking. In this test program, the problem is only seen in three cases, Bi\_01\_4, Bi\_01\_5 and Bi\_01\_6.

As a summary, the quality of the initial part of the input wave time series (WG1-3) is very important and if it is fine the time series at WG7 (at the toe of the dike) is predicted very well.

Figure 5-5: Comparison of time series in Bi\_01\_4 case (SWASH vs Physical model)

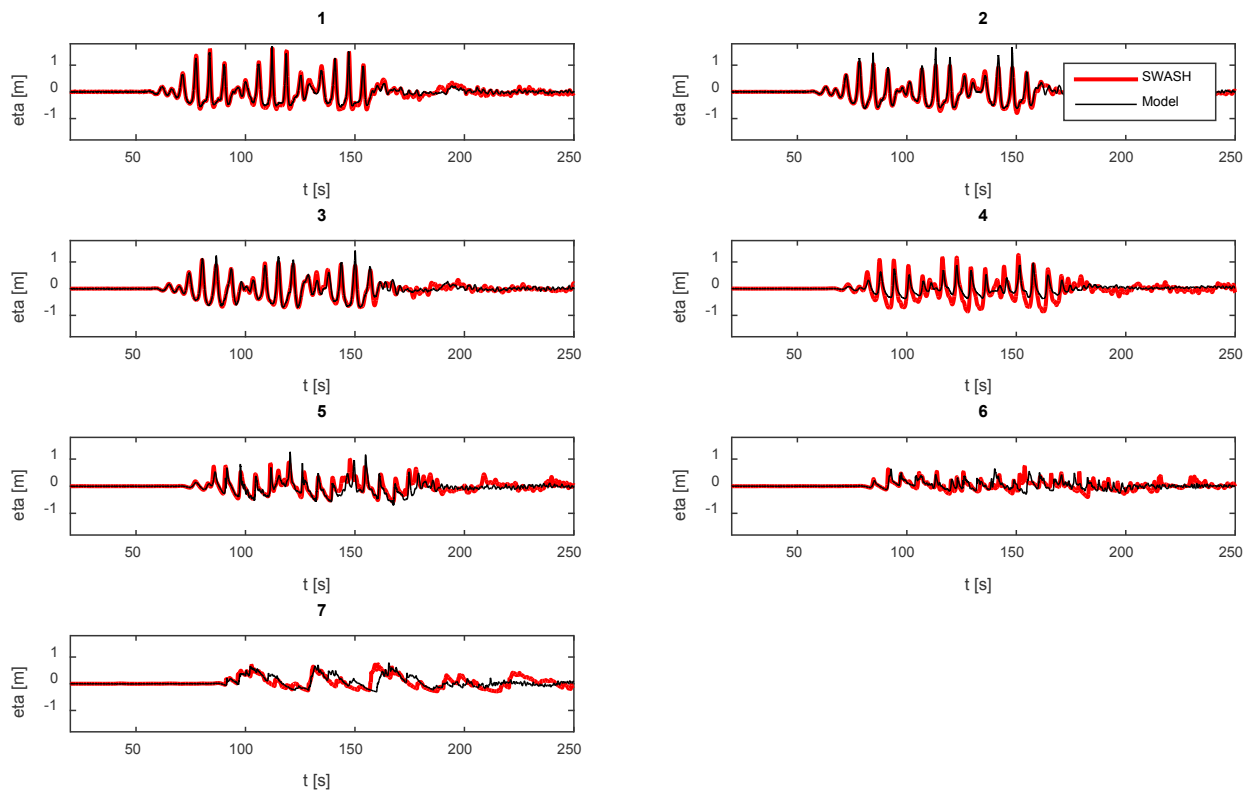


Figure 5-6: Comparison of time series in Bi\_02\_6\_R case (SWASH vs Physical model)

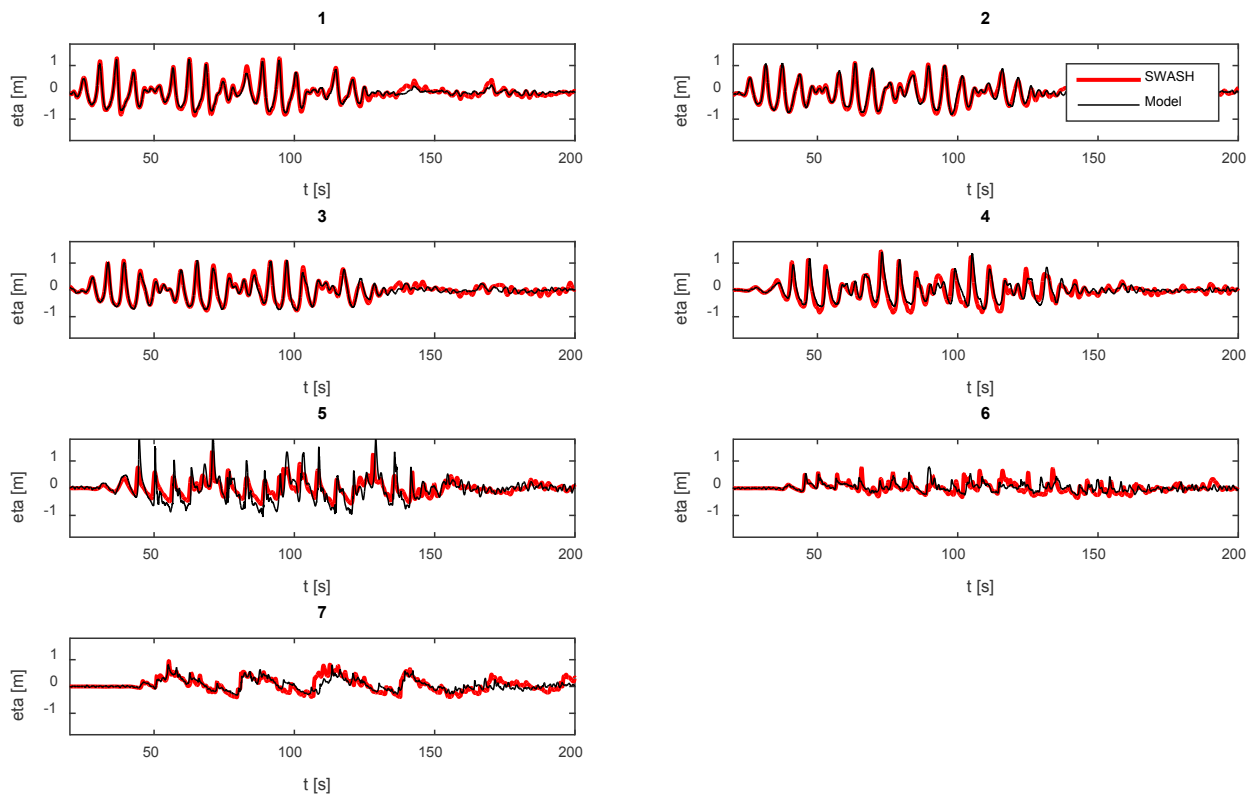
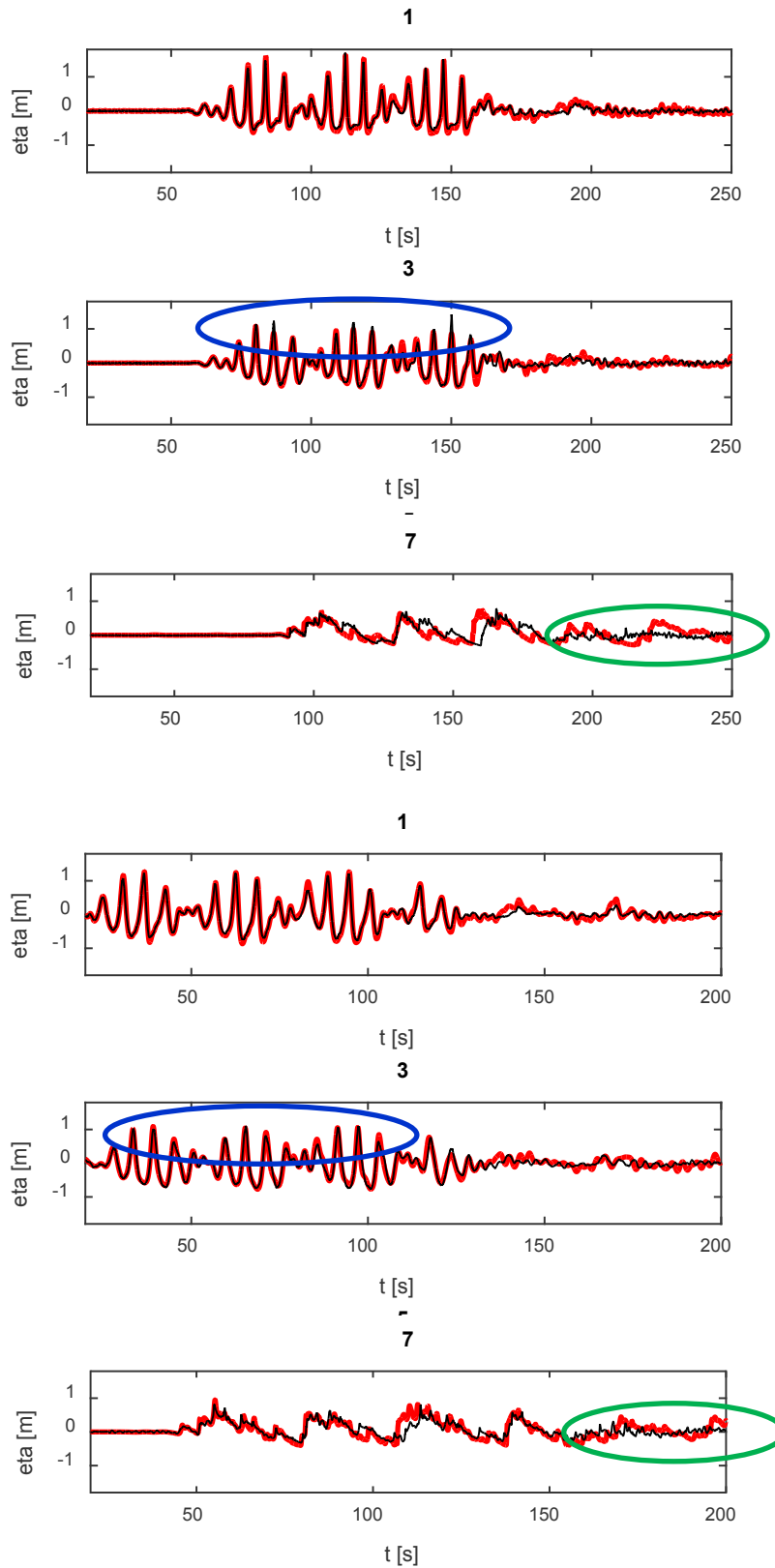


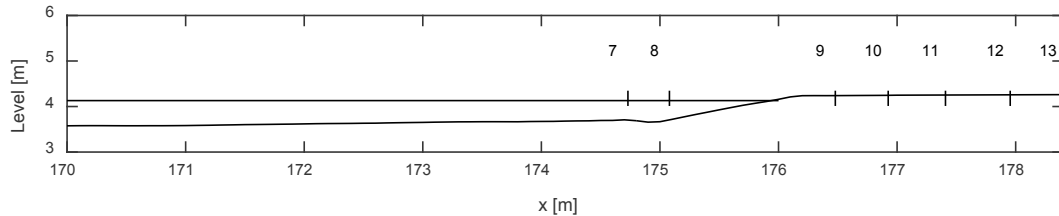
Figure 5-7: Quality of time transformation from WG1 to WG3 between 'good' case (upper 3 panels) and 'excellent' case (lower 3 panels) and WG7s.



## Wave transformation on the dike and wave force estimation

In this section wave transformation on the dike (from WG7 to WG12 in SWASH, see Figure 5-8) and force estimation are discussed.

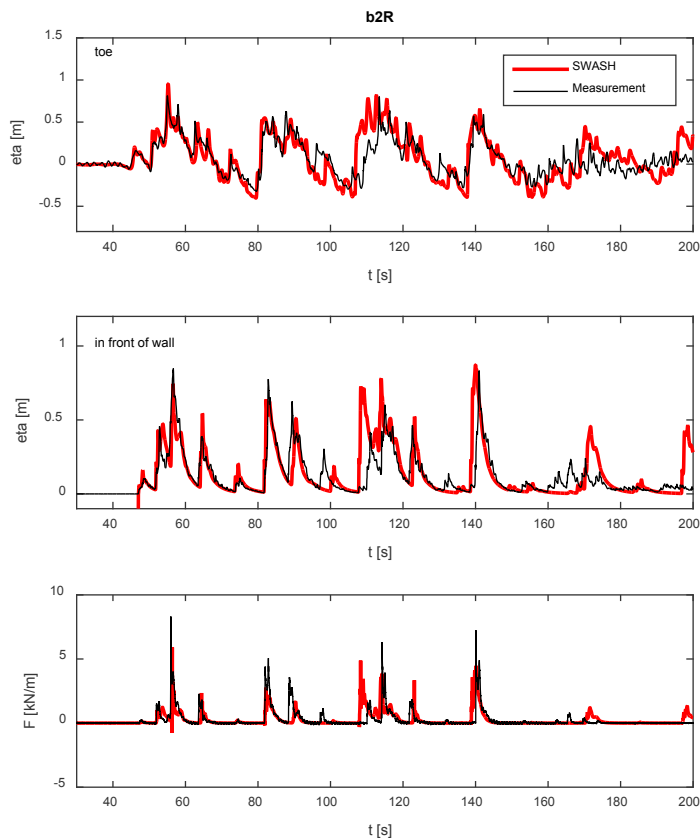
Figure 5-8: WG position on the dike in SWASH



9-12 are WGs to measure layer thickness in SWASH.

The wave transformation on the dike and force estimation from the 'excellent' case in the previous section is shown in Figure 5-9 (case Bi\_02\_6\_R). As can be seen a good correspondence is found between SWASH and measurement not only wave time series at toe of the dike (i.e. WG7) but also wave time series in front of the wall (i.e. WG12) and force acting on the wall.

Figure 5-9: Comparison of time series of eta and force in Bi\_02\_6\_R case (SWASH vs Physical model)



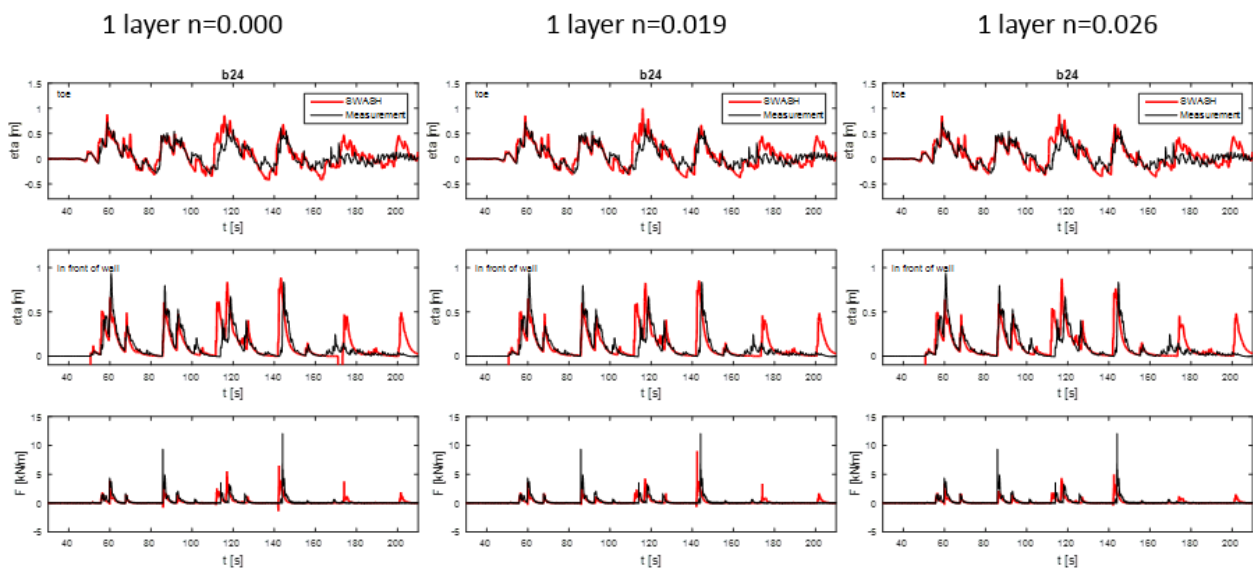
### Sensitivity analysis on bottom friction

Figure 5-10 shows comparison of wave transformation and force estimation with different bottom friction parameters.

As can be seen in the figure, there is no significant influence of bottom friction while small difference can be seen in force estimation.

From those results, it can be concluded that the influence of bottom friction is somewhat limited when the dike length (i.e. dry part) is limited. However, it is expected that the bottom friction plays an important role for wave run-up (eventually overtopping/force) when there is a long dry beach (or berm) in front of the overtopping measurement point (e.g. safety line in the safety assessment).

Figure 5-10: Comparison of wave transformation and force estimation with different bottom friction parameters.



Top figures shows wave signal at the toe, the second ones are measured on the dike and bottom ones are force measurement.

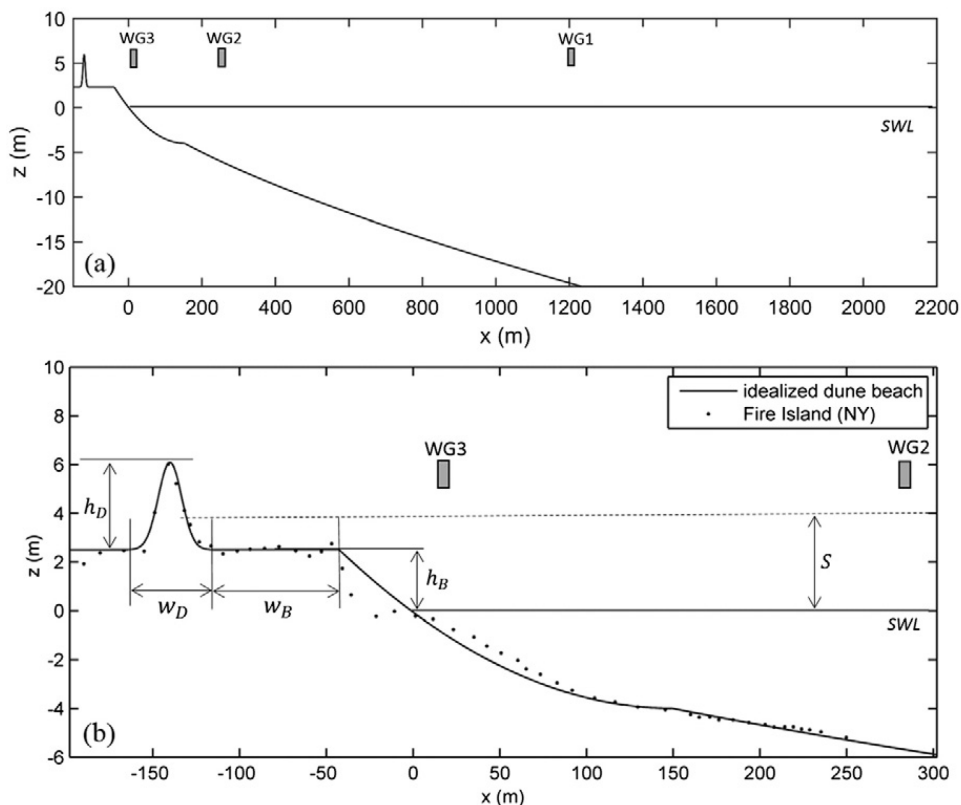
## 5.5 Park & Cox

### 5.5.1 Model settings

Figure 5-11 illustrates an example of the idealized profile defined by Park & Cox (2016). They developed a simplified dune–berm profile based on the assumptions that the berm width is flat and that the dune follows a Gaussian shape. The beach profile is based on an equilibrium beach profile which Romańczyk et al. (2005) defined. In principle the beach slope is determined by d50 size of sand. Park & Cox's study consists of 3 cases. The first one, namely Case 1A-1C, is a fixed surge level case and does not use the berm and dune but only extension of the foreshore slope on the dry beach following Romańczyk et al. (2005). The second uses the same bathymetry but uses different surge levels and the third one uses the berm and dunes.

Our study only uses only the first case (i.e. Case 1A-1C) for two reasons. First, the third case of Park & Cox's study (using berm and dune) is based on only their numerical model, so the proposed equation might be including some model effects. On the other hand Case 1A-1C compare with empirical equations based on field measurement and physical model tests in literature, and therefore the case is more reliable. Secondly the 1A case still has a relatively long run-up distance (c.a. 50 m) and this is similar dry beach distance for our application (cfr Knokke beach nourishment project). Therefore the berm and dune configuration defined in the third case is not necessary to be used.

Figure 5-11: Example of numerical model bottom setting in Pax&Cox's study



$B=3.5\text{m}$ ,  $S=0\text{m}$ ,  $w_B=0\text{m}$ ,  $h_D=0\text{m}$ ,  $w_D=0\text{m}$  in Case 1A-1C

The tested parameters for Case 1A-1C are listed below in combination with Table 5-4. In total around 400 runs have been conducted. Note that some cases are not successfully executed due to instability of the SWASH runs.

- Bottom friction:  $n=0.000, 0.019$  and  $0.025$
- Number of calculation layers in SWASH: 1 layer and 2 layers
- Wave generation: First order and Second order waves (only sub-harmonic)

Table 5-4: Test conditions for Case 1A-1C

Case	$D_{50}$ [mm]	$\tan \beta_f$ [-]	$H_s$ [m]	$T_p$ [s]
1A	0.3	0.023	1.0, 2.0	10, 12.5, 15, 17.5
1B	0.4	0.054	1.0, 2.0	10, 12.5, 15, 17.5
1C	0.5	0.091	1.0, 2.0	10, 12.5, 15, 17.5

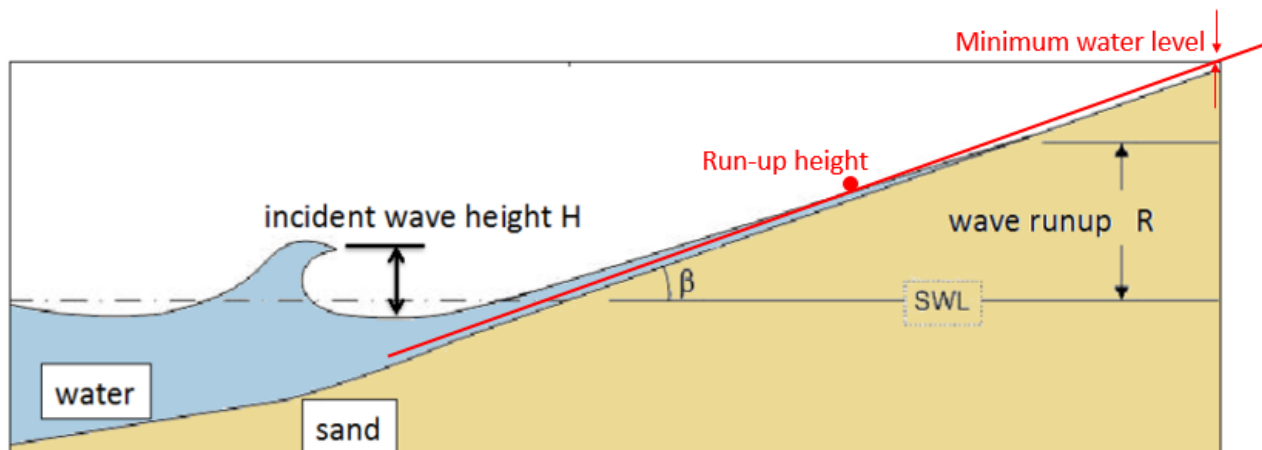
### 5.5.2 Implementation of time dependent wave run-up value in SWASH

Park & Cox's study focused on wave run-up. However the present SWASH model (version 4.01) does not have a function to output time dependent wave run-up value (from which representative wave run-up parameter can be calculated, e.g. R2%), while which only has output of maximum wave run-up value (i.e. Rmax) during the entire run. Therefore in this study the time-dependent wave run-up value is implemented in SWASH version 4.01. Note that this implementation will be officially released in the future SWASH version including 2DH (i.e. basin like) application, however this implementation is only limited to 1D (2DV; i.e. flume like) application at this moment.

The algorithm is shown as follows.

- 1) Decide run-up criteria value (height above the bottom level). Note that Fiedler et al. (2018) uses 0.1 m as the run-up criteria.
- 2) Detect the first grid point from the last calculation grid in x direction which exceeds the run-up criteria.
- 3) Calculate exact run-up value from the equation below (run-up criteria 0.01 is used in the equation).
- 4) Output wave run-up value at each time step.

Figure 5-12: Wave run-up criteria (i.e. minimum water level)



### 5.5.3 Post-processing of wave run-up calculation results

Output example of the time series of the wave run-up is shown in Figure 5-13. As can be seen, time series present some noise close to each crest level. The reason of the noise could be originated due to numerical issue but the exact reason has not been understood yet. For an easier processing of the signal, a low-pass filter is applied after some testing with different frequencies. Eventually, a low-pass filter of 0.1 Hz gives a reasonable output (as shown with red line in Figure 5-13) while it gives some small underestimation. We accept this underestimation as a model effect. Figure 5-14 shows an output example of spectrum at three wave gauge locations in the numerical domain as defined in (Park & Cox, 2016) and entire and part of wave run-up time series. As can be seen, all the run-up points are well captured thanks to the post-processing (i.e. smoothing through the low pass filter).

Figure 5-13: Output example of wave run-up time series (blue) and smoothed one (red)

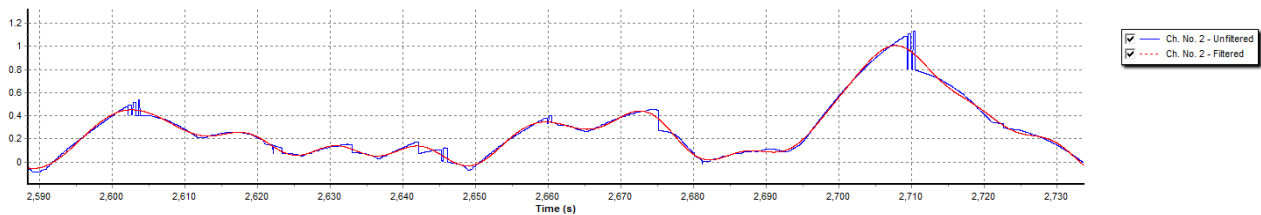
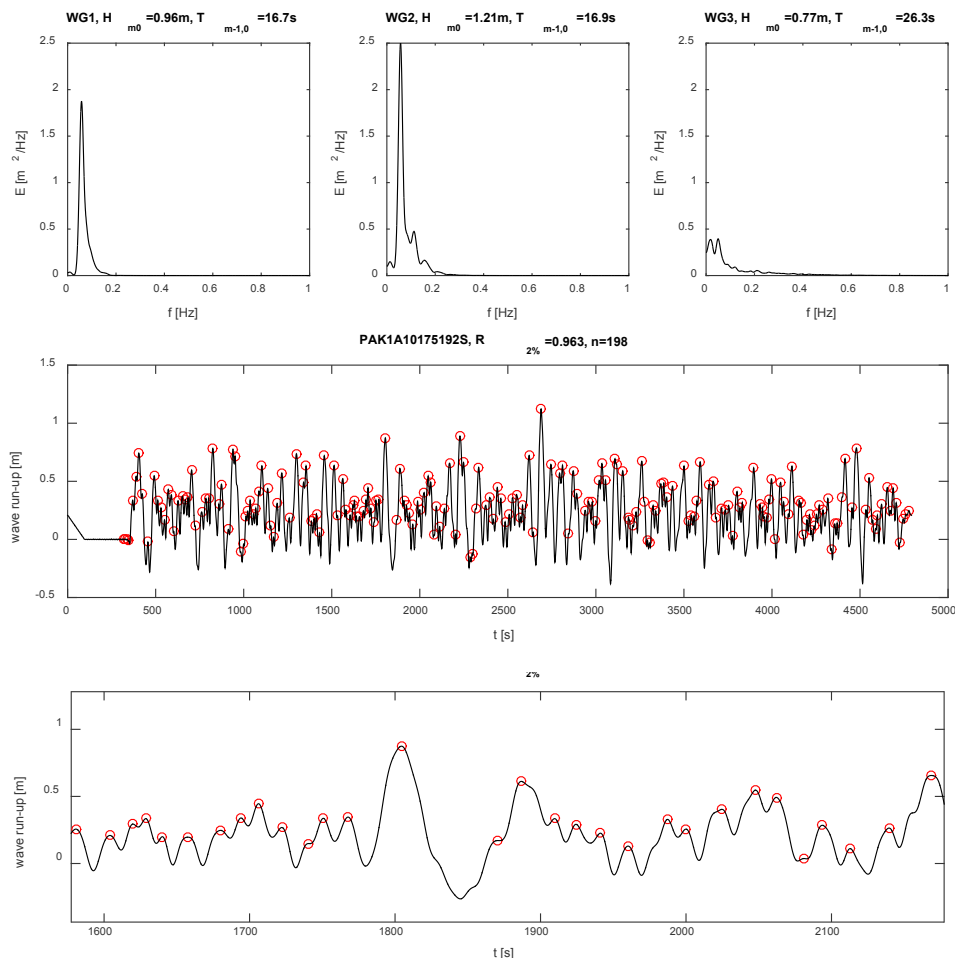


Figure 5-14: Output example of spectrum at three wave gauge locations and entire and part of wave run-up time series



### 5.5.4 Results

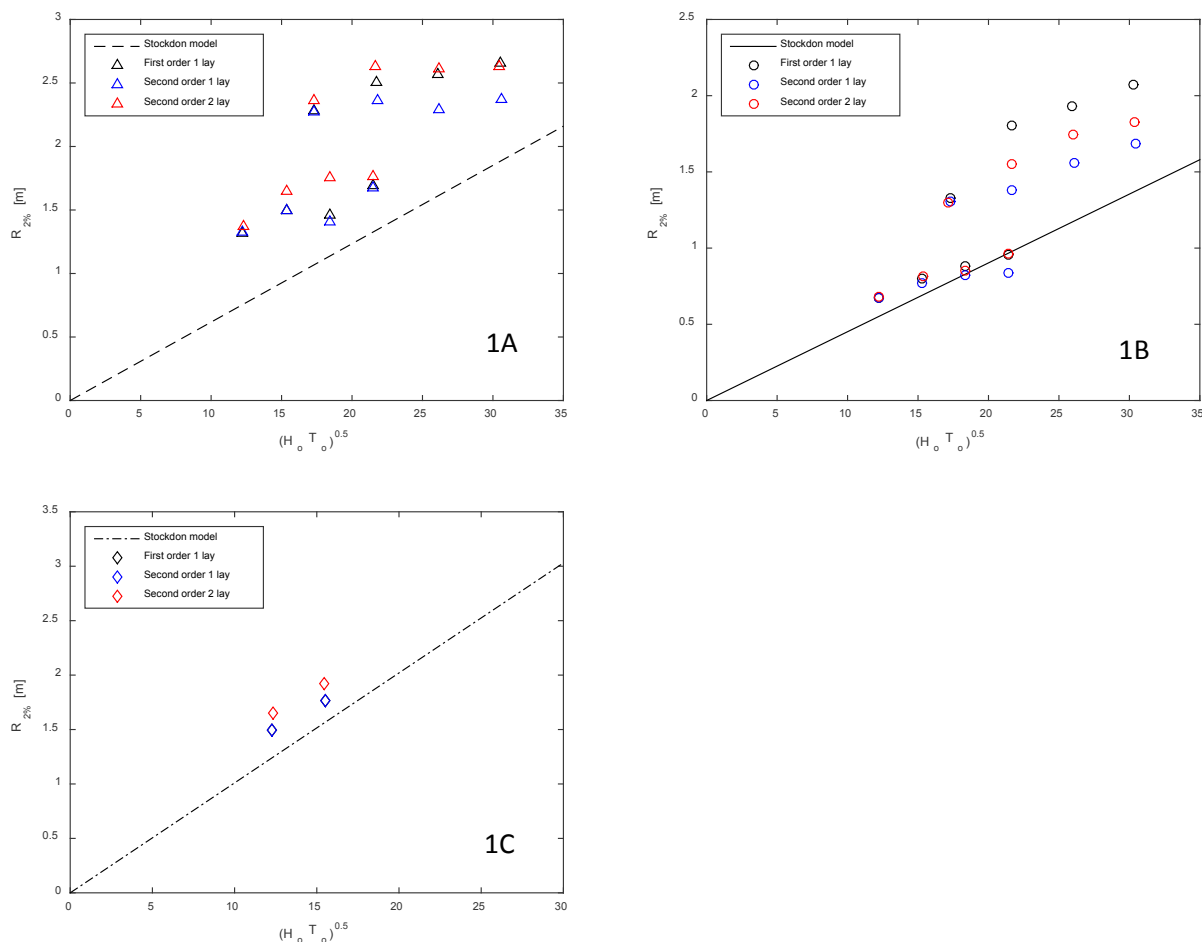
Park & Cox conducted three comparisons with empirical equations. One is with the Stockdon model. The other ones are with Mase and Holman models. The results are shown below.

#### Comparison with Stockdon model

Figure 5-15 shows SWASH wave run-up result R2% comparing with empirical equation developed by Stockdon. Generally wave run-up estimated in SWASH is overestimated compared to Stockdon model which is based on field measurement. This means that the Stockdon model includes directional spreading effect while SWASH model is conducted in 1D (i.e.2DV). Therefore the difference can be explained by the directional spreading effect. However, unfortunately, in this study 2DH calculation cannot be conducted due to the limitation of the implementation of run-up in SWASH at this moment.

The observation of the different outputs of SWASH is described here below (i.e. First order wave generation with 1 layer, second order in 1 layer and second order 2 layers). First of all, SWASH 1st order wave generation results give the highest wave run-up (up to 30%). This is due to spurious long wave generation which has been observed in Wenduine physical model test. This spurious long wave can be restricted by 2<sup>nd</sup> order wave generation in theory. However according to Rijsdorp et al. (2014), 2<sup>nd</sup>-order wave generation with 1 layer also includes some spurious free energy and this can be improved by using more than 2 layers. As shown in the result, indeed SWASH 2nd order wave generation in 2 layer give some differences in run-up compared to one from 2nd order wave generation in 1 layer (up to 15 % difference).

Figure 5-15: SWASH wave run-up result vs Stockdon model (n=0.019)

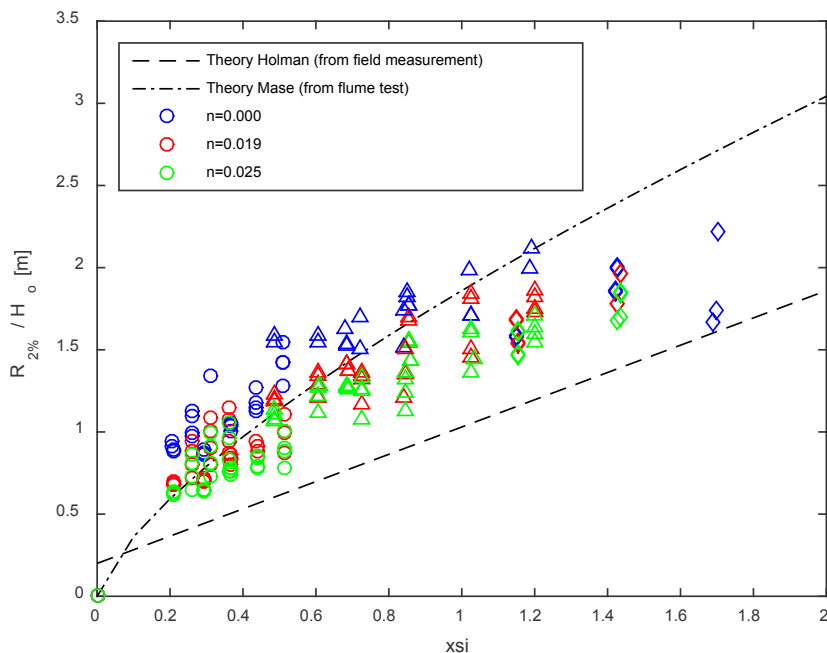


### Comparison with Mase and Holman model

Figure 5-16 shows comparison of normalized wave run-up between SWASH and two empirical models, Mase and Holman. Mase's model is developed based on their 2DV flume test while Holman's model is developed based on field measurement. As stated above, directional spreading effect again plays an important role. As can be seen in the figure, cloud of the SWASH results is closer to Mase's model due to directional spreading effect. SWASH results consist of 3 different bottom friction values,  $n=0.000$ ,  $0.019$  and  $0.025$ . In line with the other flume test (i.e. the bottom is impermeable smooth material), the bottom friction parameter for the physical model from Mase would be around  $0.012$ . The result shows that Mase's model comes in between SWASH results of  $n=0.000$  and  $n=0.019$ . This implies that the SWASH performance is promising. Even if we did not conduct the case with  $n=0.012$  in SWASH, it would presumably give a good fit to the empirical equation line.

One conclusion that can be drawn from this result is that material based  $n$  values give a good estimation in this case.

Figure 5-16: Comparison of normalized wave run-up between SWASH and empirical models



The spreading for constant  $\xi$  value is caused by different settings of the SWASH runs (1<sup>st</sup> order and 2<sup>nd</sup> order, one layer and two layers)

## 5.6 Further discussion of Fielder et al. (2018)

As can be seen, SWASH performance is promising in the tested cases (Wenduine, Chen, ICODEP, WaLoWa and Mase), and there are obvious directional spreading effect in 1D calculation. However, Fielder's result indicates there is no directional spreading effect (1D calculation represents the wave run-up almost perfect: with error of 6-8 % error). We do not still understand the mechanism why Fiedler's 1D SWASH model fits to field data. Even they mention that the 2D dynamics that lead to good 1D model performance are not understood (see details below).

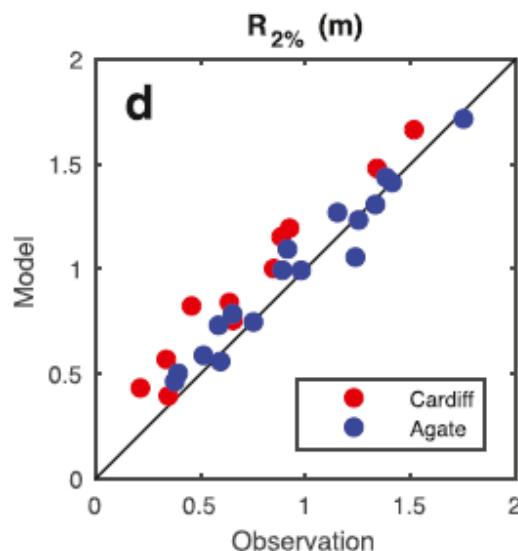
### 4.6. 1D vs 2D domains

The 1D SWASH model (normally incident SS and IG waves) neglects wave obliquity and directional spread, with the benefit of reduced computational time. Furthermore, SWASH 1D yields runup results that agree well with the data without any significant changes to the default model parameters. However, bulk runup statistics in the 2D numerical model funwaveC depend on directional spread (Guza and Feddersen, 2012), equal to 0 in the 1D model. Preliminary SWASH 2D results are qualitatively similar to SWASH 1D. Unfortunately, artifacts of the 2D model geometry can preferentially excite certain edge wave and seiche-like modes, and 2D SWASH results are not presented here. The 2D dynamics that lead to good 1D model performance are not understood.

We are not sure but in general field data contains a lot of uncertainties (e.g. bathymetry is not taken during the storm), so it is interesting to investigate this directional spreading effects in a physical model test. This project is ongoing within the CREST project (WL project number 18\_039).

Looking into some more details of their result, Figure 5-17 still indicates that directional spreading is playing an important role: Cardiff case (directional spreading of 20 deg) is a bit more overestimating run-up compared to the one in Agate (10 deg). As stated above detailed investigation of directional spreading effect will be studied soon in the CREST project.

Figure 5-17: Estimation of wave run-up conducted by Fiedler et al. (2018)



## 6 Conclusions

### 6.1 Bottom friction n value

This study indicates that material based n value gives good estimation for wave transformation and run-up, for all the tested cases.

Taking into account the fact that the Manning coefficient for the sand and promenade material would be around 0.019, the default bottom friction value  $n=0.019$  is recommended for overtopping calculation in SWASH. Note that the value can be changed if the material's n is much differ from  $n=0.019$ .

### 6.2 Wave generation and number of waves

SWASH 2nd order wave generation in 2 layer give some differences in run-up compared to one from 2nd order wave generation in 1 layer (up to 15 % difference). The difference is not that big in the tested configuration while (more than) 2 layers are supposed to be more accurate in terms of wave generation as mentioned by Rijdsdorp et al. (2014). It is noted that this might cause instability problem since in general 2 layers are more unstable than 1 layer. Further validations (e.g. using the 2DH physical model test in CREST project) will be useful in order to select a robust method.

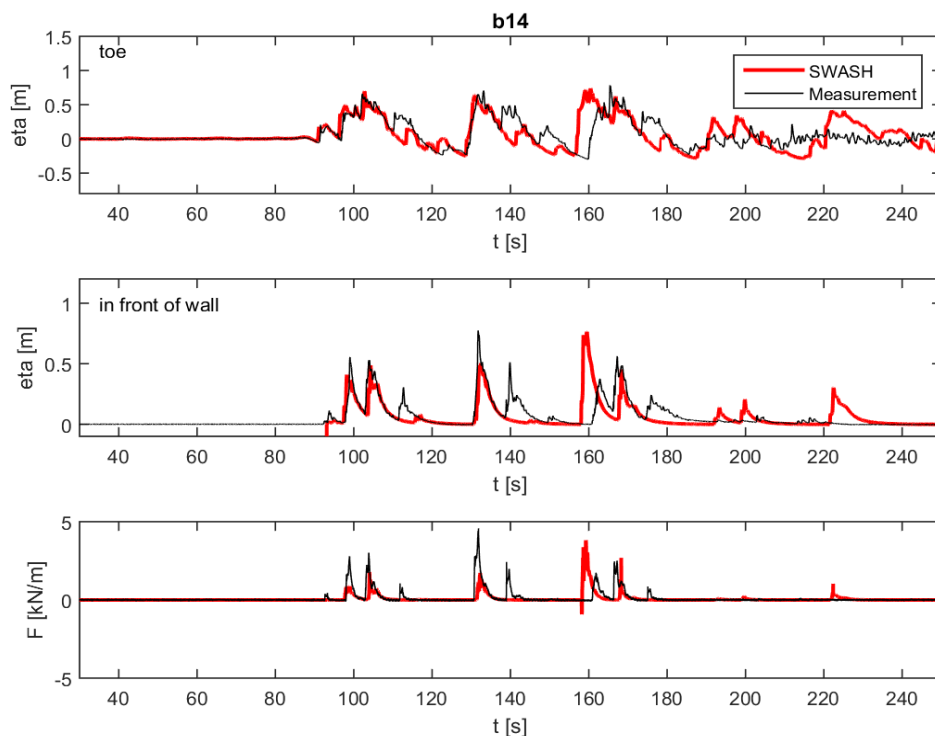
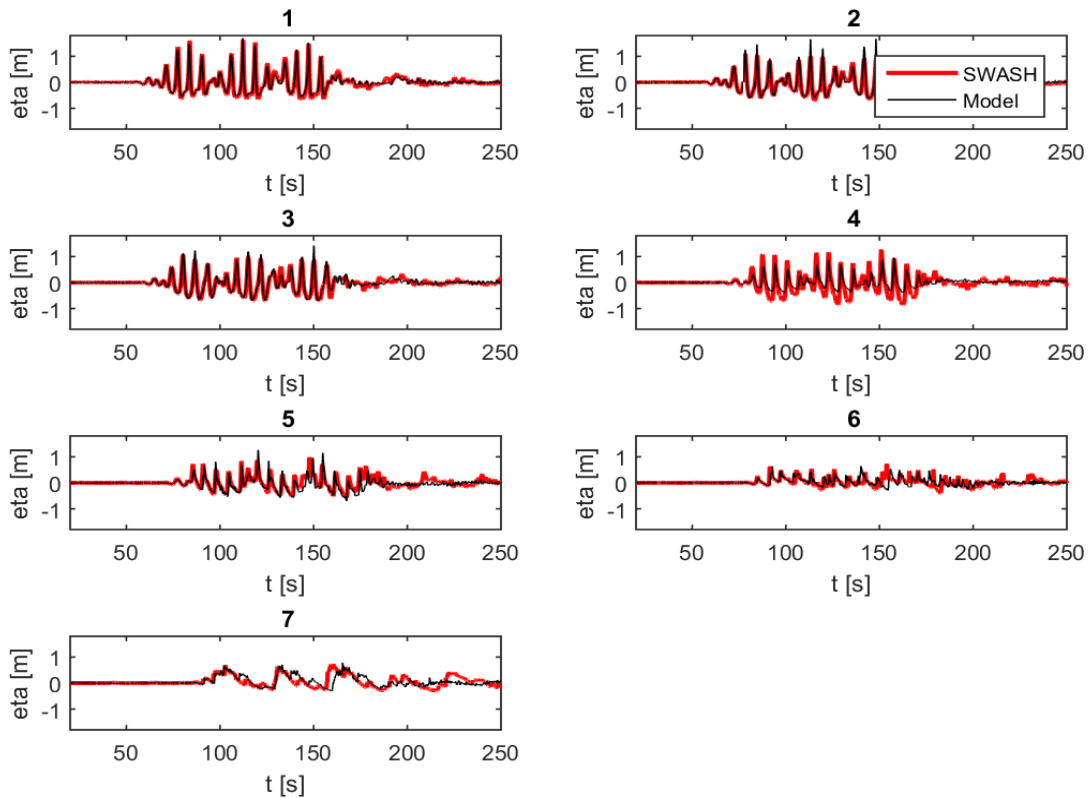
## References

- Allsop, N.W.H.; Bruce, T.; De Rouck, J.; Kortenhaus, A.; Pullen, T.; Schüttrumpf, H.; Troch, P.; Van der Meer, J.W.; Zanuttigh, B.** (2016). EurOtop II. Available at: [www.overtopping-manual.com](http://www.overtopping-manual.com)
- Altomare, C.; Suzuki, T.; Chen, X.; Verwaest, T.; Kortenhaus, A.** (2016). Wave overtopping of sea dikes with very shallow foreshores. *Coast. Eng.* 116: 236–257. doi:10.1016/j.coastaleng.2016.07.002
- De Waal, J.P., Van der Meer, J.W.** (1992). Wave run-up and overtopping on coastal structures. *Coast. Eng. Proc.* 1 (23), 1758–1774.
- Fiedler, J.W.; Smit, P.B.; Brodie, K.L.; McNinch, J.; Guza, R.T.** (2018). Numerical modeling of wave runup on steep and mildly sloping natural beaches. *Coast. Eng.* 131: 106–113. doi:10.1016/j.coastaleng.2017.09.004
- Holman, R.A.** (1986). Extreme value statistics for wave run-up on a natural beach. *Coast. Eng.* ISBN 03783839 (ISSN) 9(6): 527–544. doi:10.1016/0378-3839(86)90002-5
- Mase, H.** (1989). Random wave runup height on gentle slope. *J. Waterw. Port Coast. Ocean Eng.* 115(5): 649–661
- Park, H.; Cox, D.T.** (2016). Empirical wave run-up formula for wave, storm surge and berm width. *Coast. Eng.* ISBN 0378-3839 115: 67–78. doi:10.1016/j.coastaleng.2015.10.006
- Rijnsdorp, D.P.; Zijlema, M.** (2016). Simulating waves and their interactions with a restrained ship using a non-hydrostatic wave-flow model. *Coast. Eng.* 114: 119–136. doi:10.1016/j.coastaleng.2016.04.018
- Smit, P.; Zijlema, M.; Stelling, G.** (2013). Depth-induced wave breaking in a non-hydrostatic, near-shore wave model. *Coast. Eng.* 76: 1–16. doi:10.1016/j.coastaleng.2013.01.008
- Stelling, G.S.; Duijnmeijer, S.P.A.** (2003). A staggered conservative scheme for every Froude number in rapidly varied shallow water flows. *Int. J. Numer. Meth. Fluids* 1329–1354
- Stockdon, H.F.; Holman, R.A.; Howd, P.A.; Sallenger, A.H.** (2006). Empirical parameterization of setup, swash, and runup. *Coast. Eng.* ISBN 0378-3839 53(7): 573–588. doi:10.1016/j.coastaleng.2005.12.005
- Suzuki, T.; Altomare, C.; De Roo, S.; Kolokythas, G.K.; Vanneste, D.; Peeters, P.; Mostaert, F.** (2017a). Methodology for safety assessment 2015 - Background report on wave transformation and overtopping calculation by SWASH. *FHR reports*, 14\_014\_6. Flanders Hydraulics Research: Antwerp
- Suzuki, T.; Altomare, C.; Veale, W.; Verwaest, T.; Trouw, K.; Troch, P.; Zijlema, M.** (2017b). Efficient and robust wave overtopping estimation for impermeable coastal structures in shallow foreshores using SWASH. *Coast. Eng.* 122: 108–123. doi:10.1016/j.coastaleng.2017.01.009
- Suzuki, T.; De Roo, S.; Altomare, C.; Zhao, G.; Kolokythas, G.K.; Willems, M.; Verwaest, T.; Mostaert, F.** (2016). Toetsing kustveiligheid 2015 - Methodologie: toetsingsmethodologie voor dijken en duinen. Versie 10. *WL Rapporten*, 14\_014. Waterbouwkundig Laboratorium: Antwerpen
- van der Meer, B.J.W.; Stam, C.M.** (1993). WAVE RUNUP ON SMOOTH AND ROCK SLOPES OF 118(5): 534–550
- VanderMeer, J.W.** (1998). Wave run-up and overtopping. In: Pilarczyk, K.W. (Ed.), *Dikes and Revetments: Design, Maintenance and Safety Assessment*. AA Balkema, Rotterdam, The Netherlands, pp. 145–159.
- Van Doorslaer, K.; Rouck, J. De; Audenaert, S.; Duquet, V.** (2015). Crest modifications to reduce wave overtopping of non-breaking waves over a smooth dike slope. *Coast. Eng.* 101: 69–88. doi:10.1016/j.coastaleng.2015.02.004
- Zijlema, M.; Stelling, G.; Smit, P.** (2011). SWASH : An operational public domain code for simulating wave fields and rapidly varied flows in coastal waters. *Coast. Eng.* 58(10): 992–1012. doi:10.1016/j.coastaleng.2011.05.015

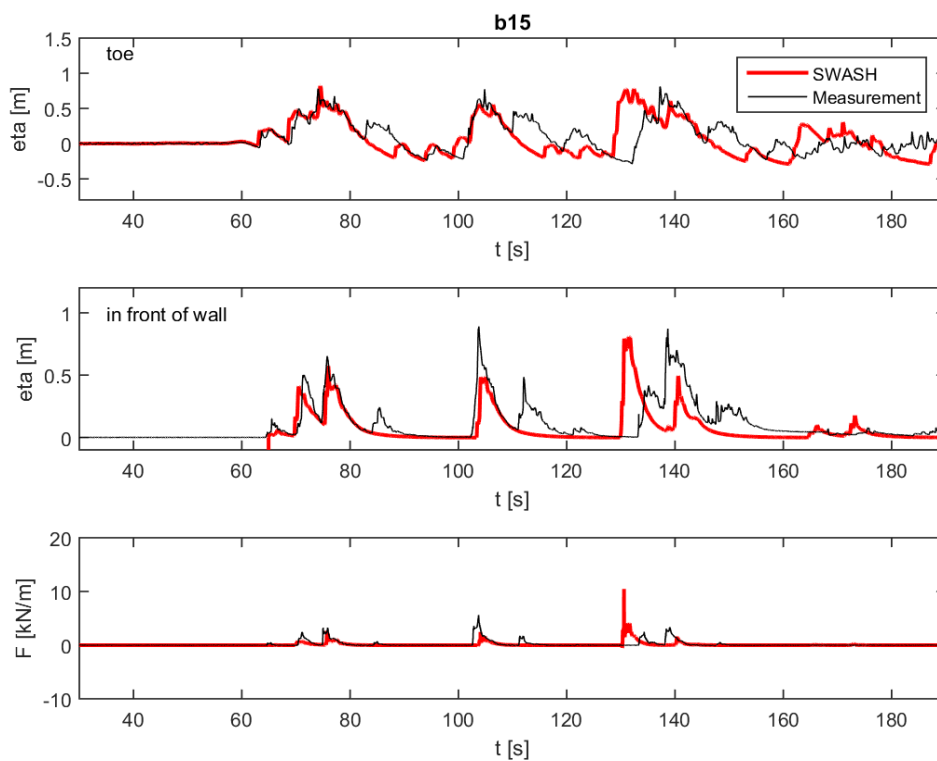
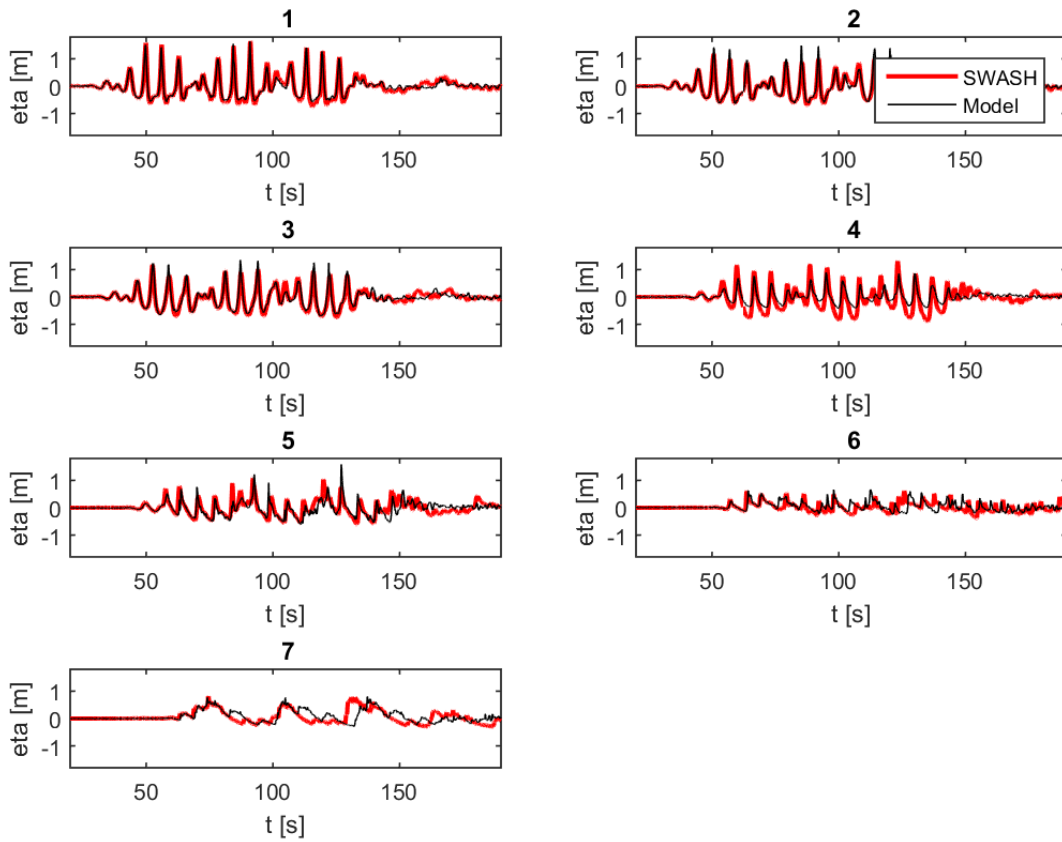
## Appendix A: WaLoWa SWASH results

All the time series (wave gauges and force) of bi-chromatic wave cases are presented here. Note that 7 in the figures indicates the time series of water surface at the toe of the dike.

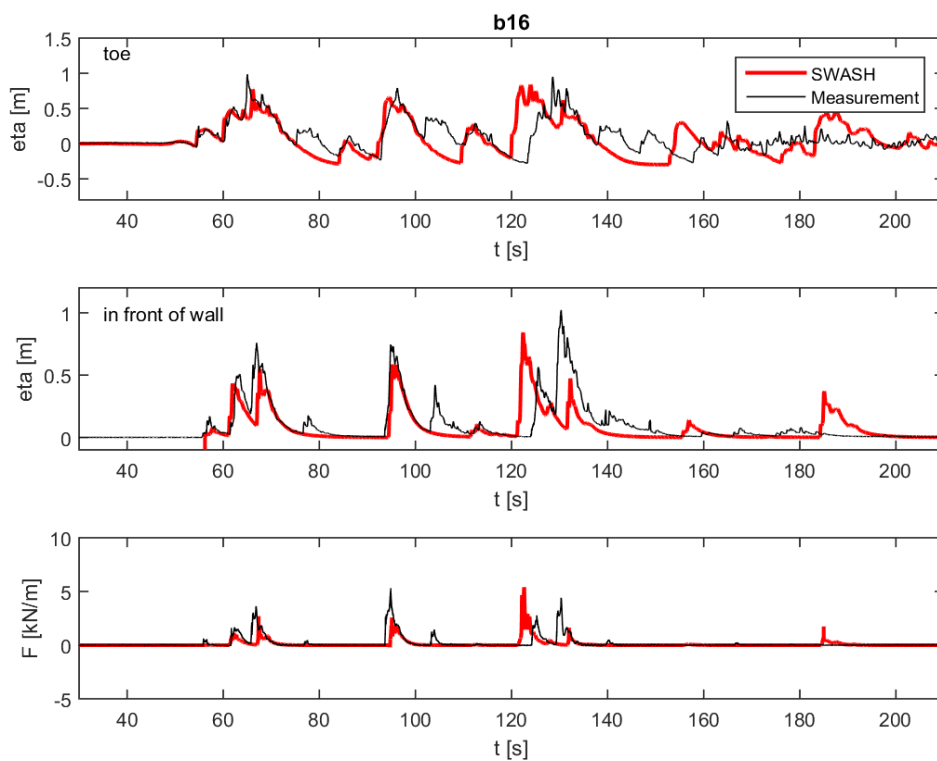
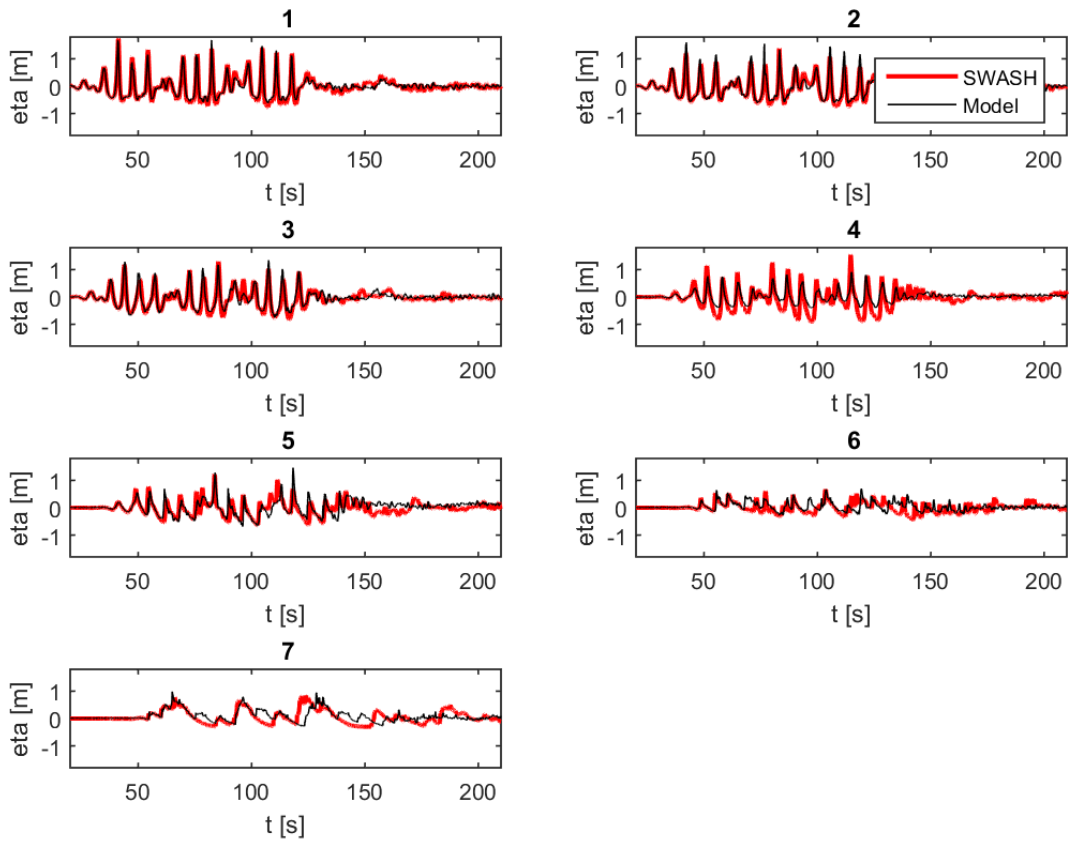
### Bi\_01\_4



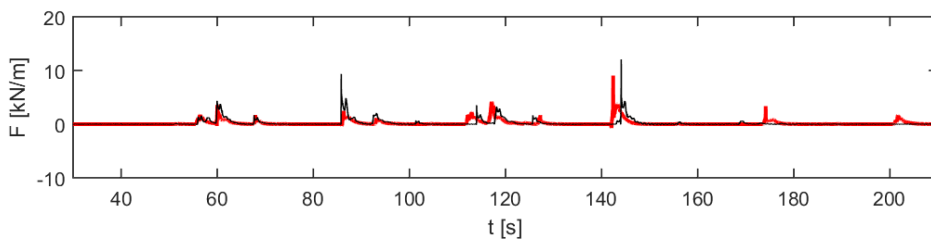
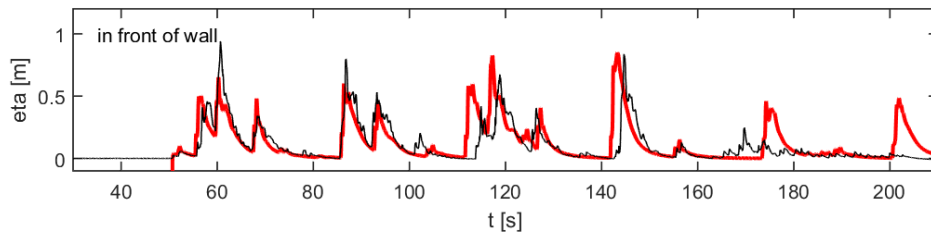
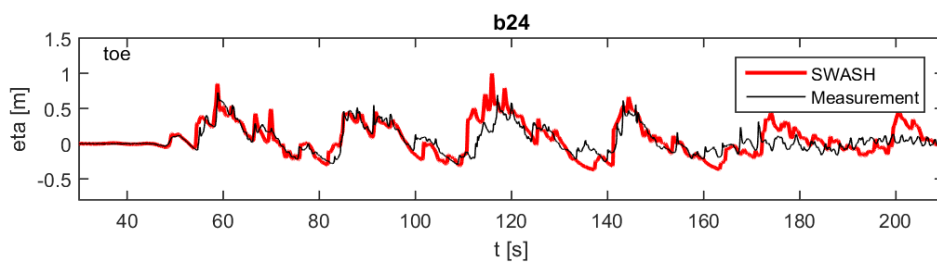
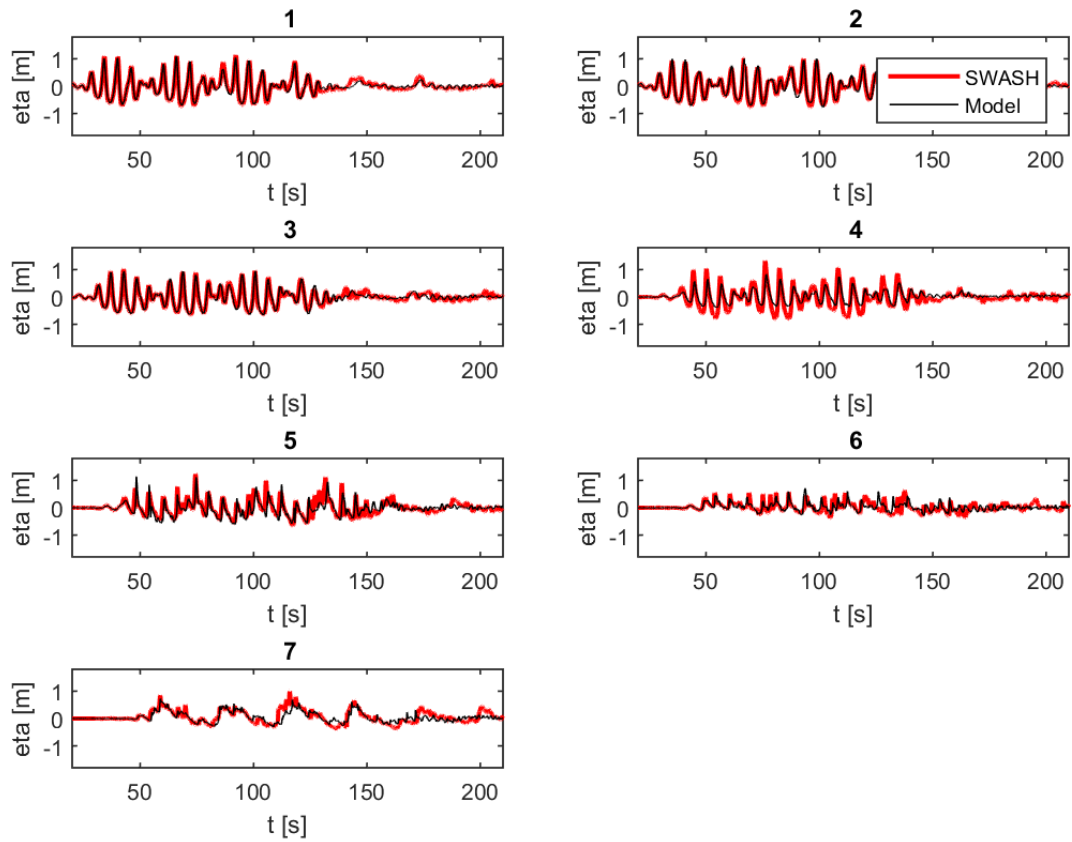
Bi\_01\_5



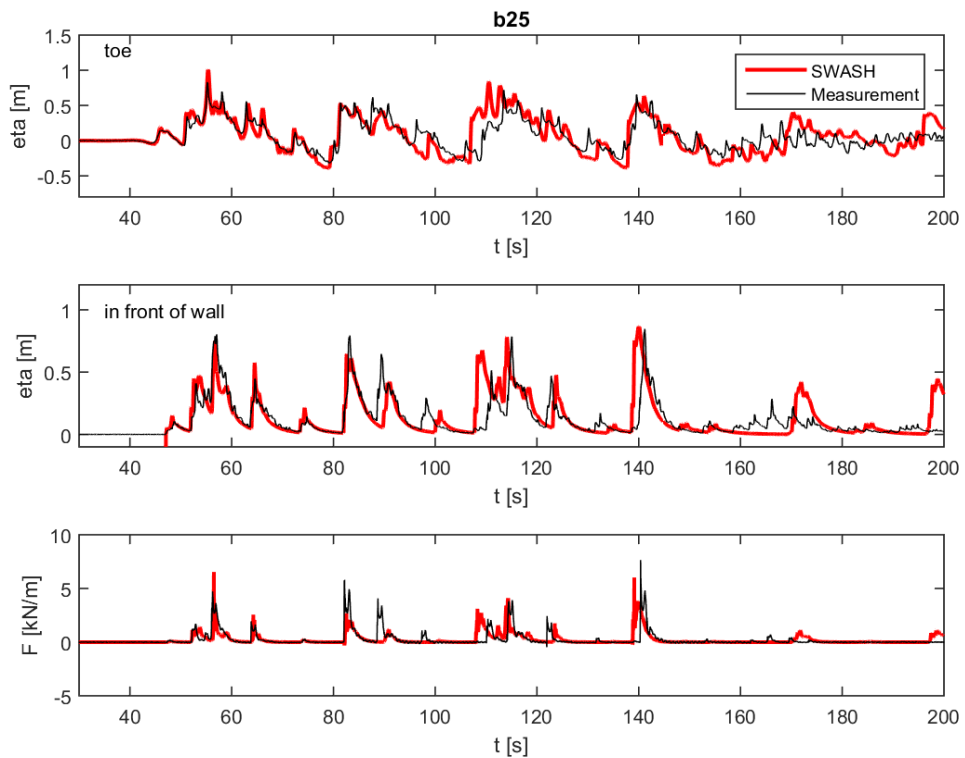
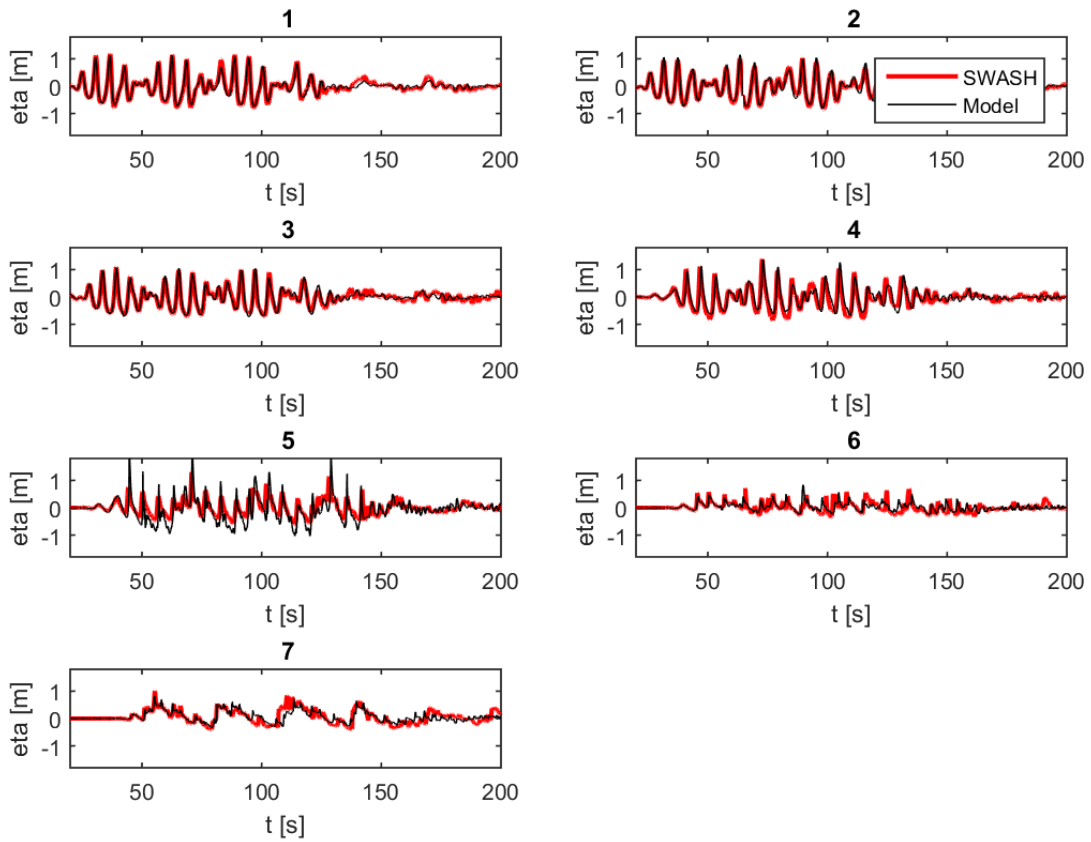
Bi\_01\_6



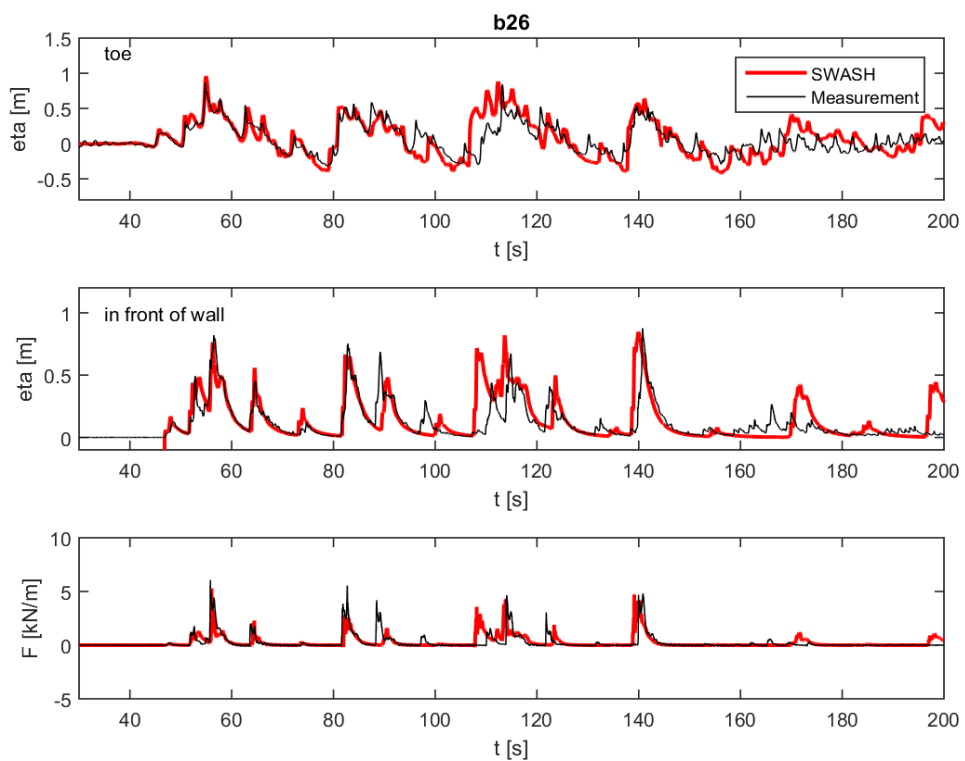
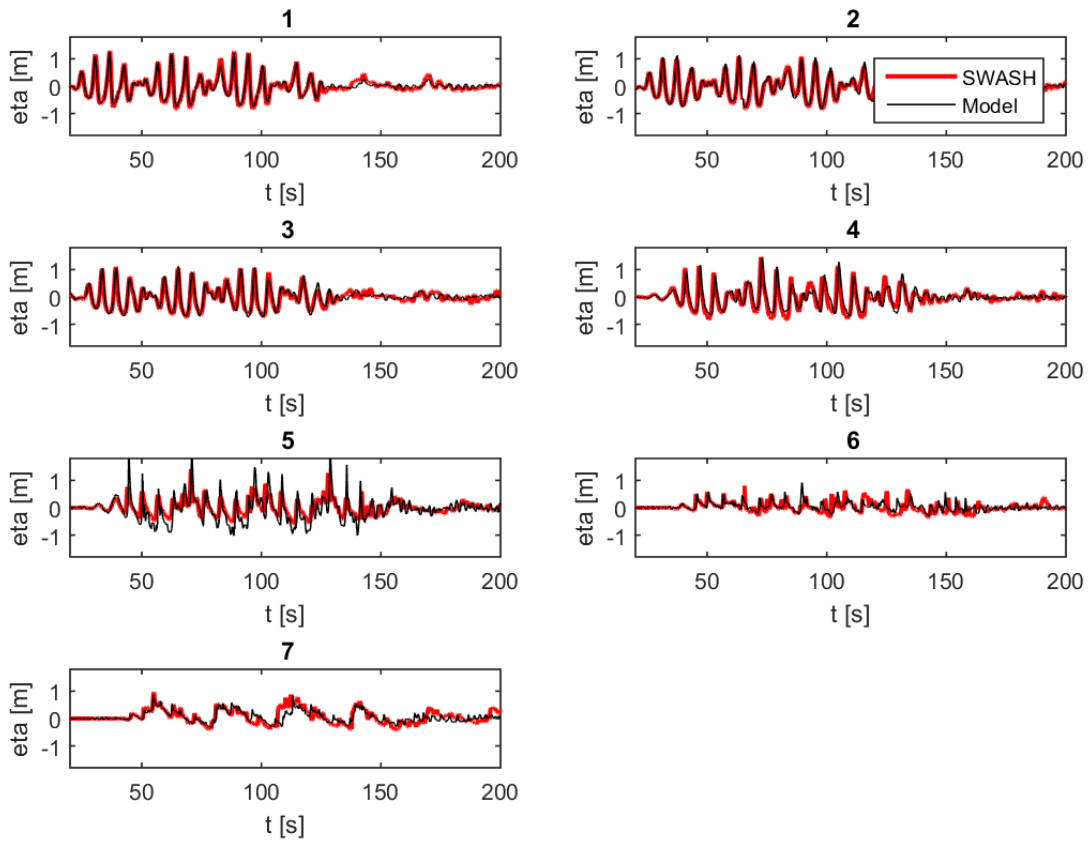
Bi\_02\_4



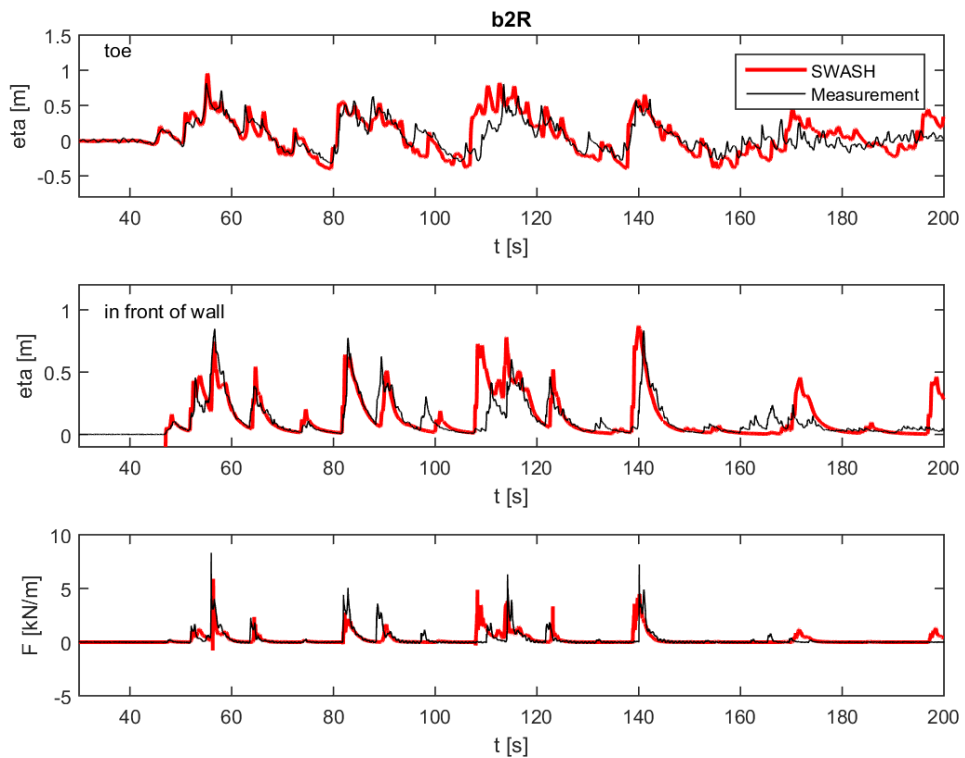
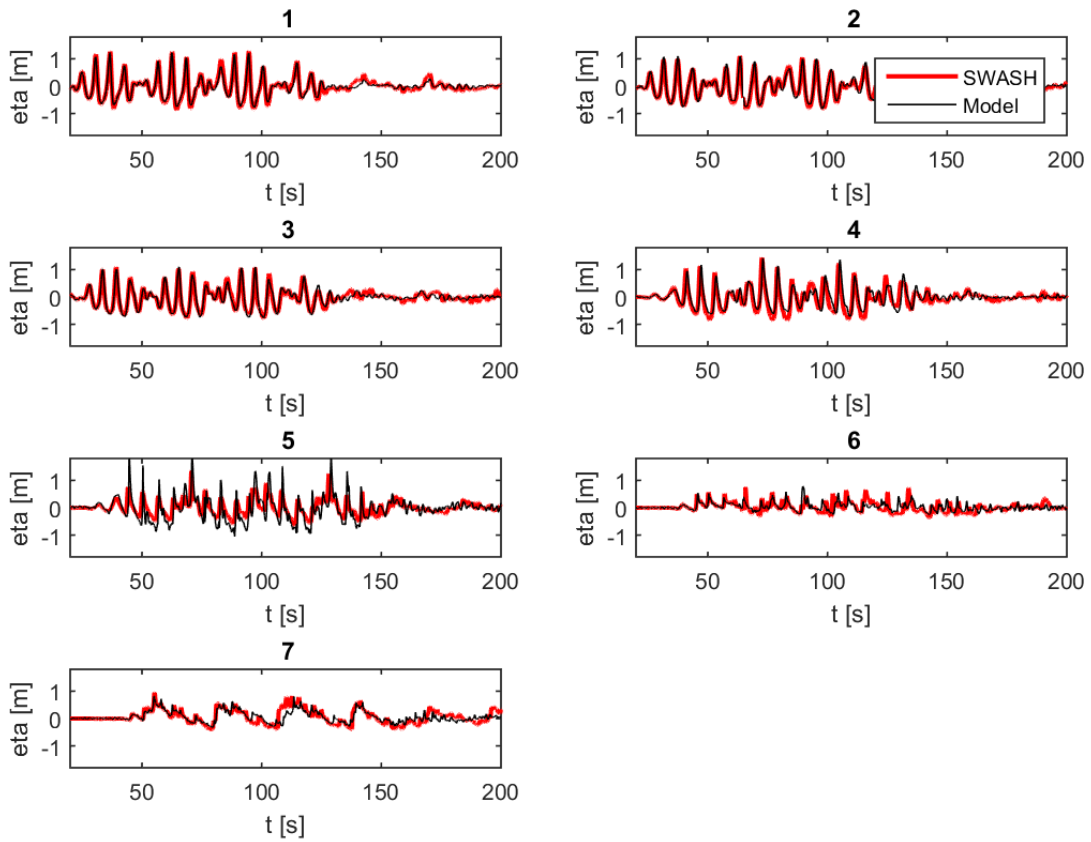
Bi\_02\_5



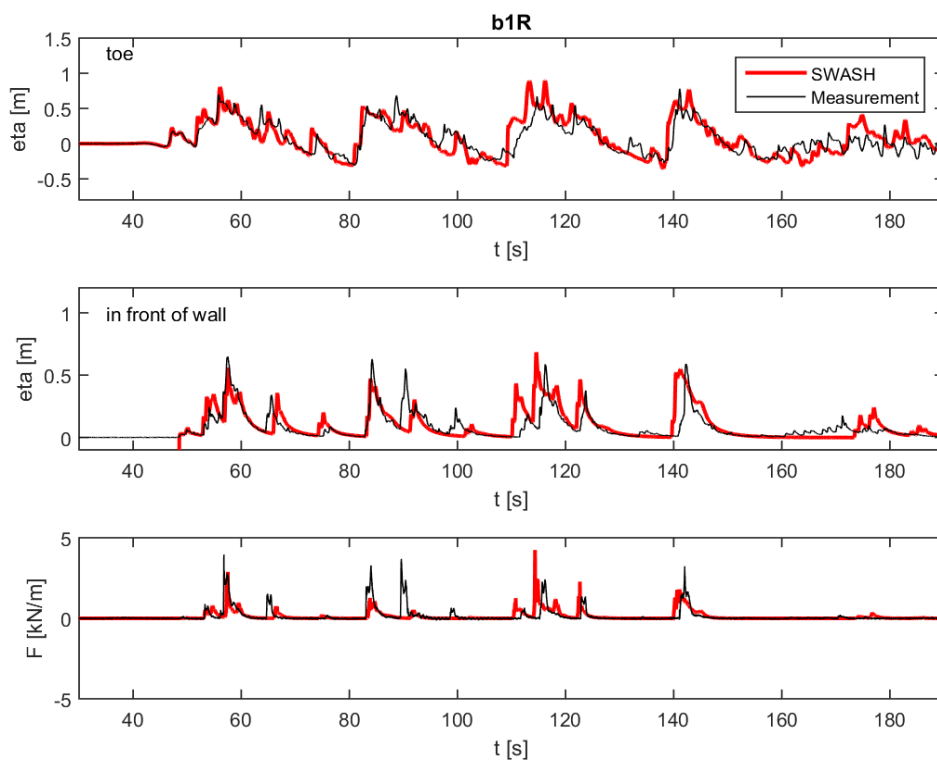
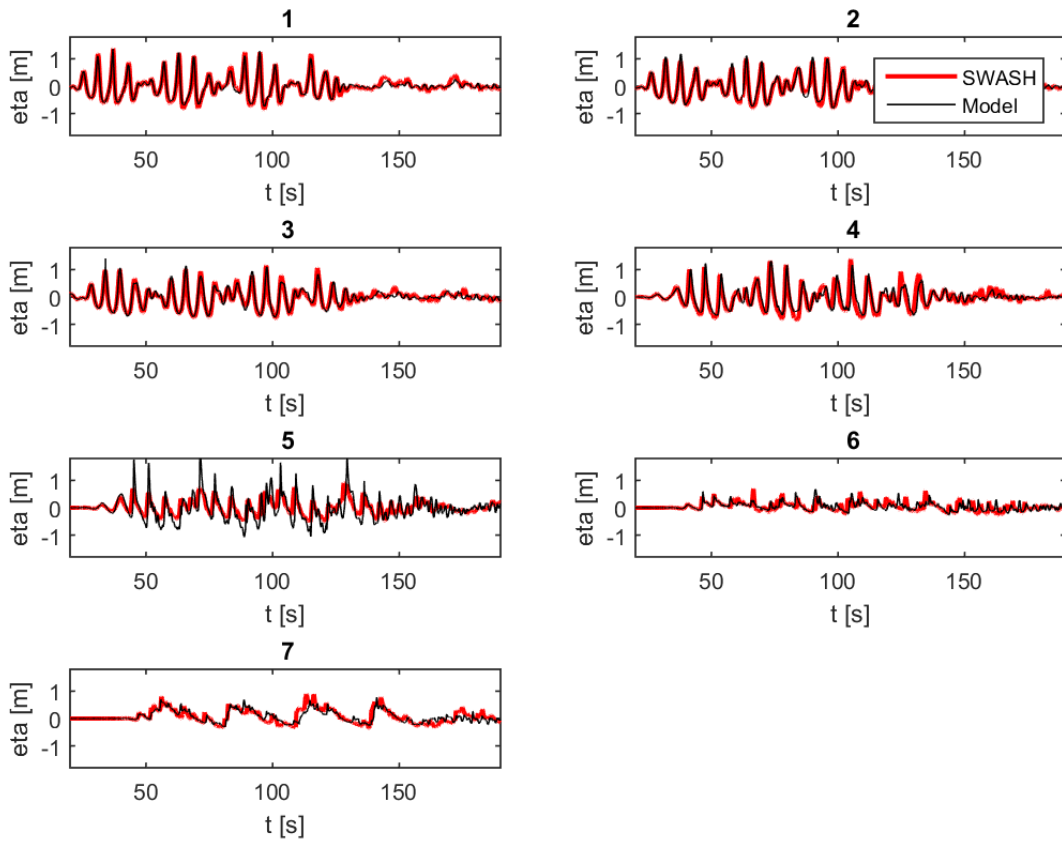
Bi\_02\_6



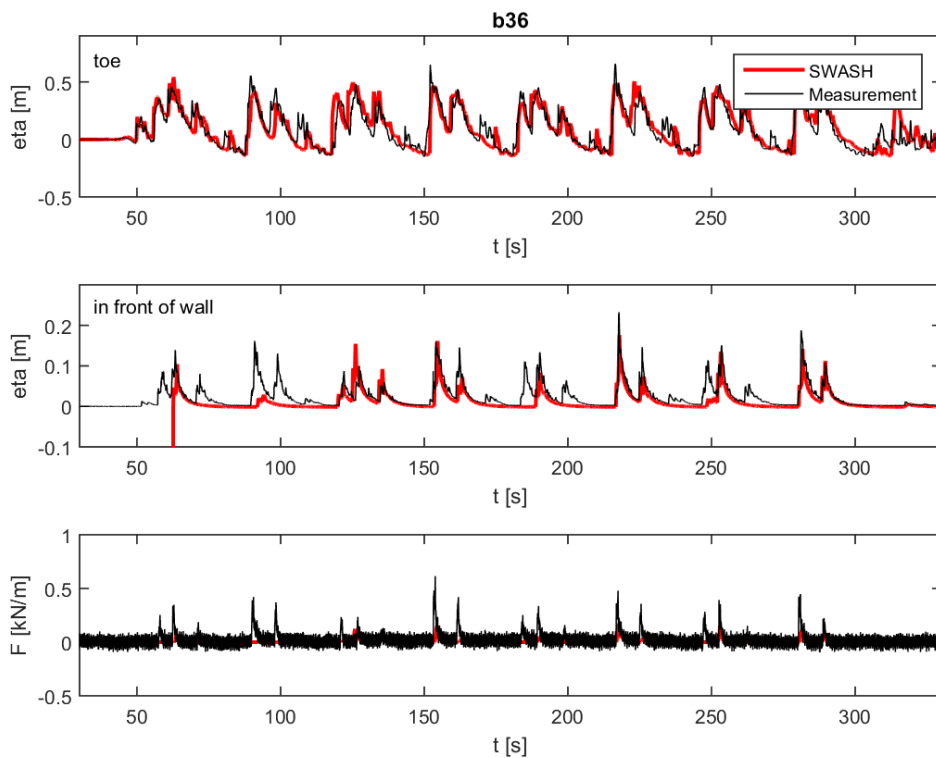
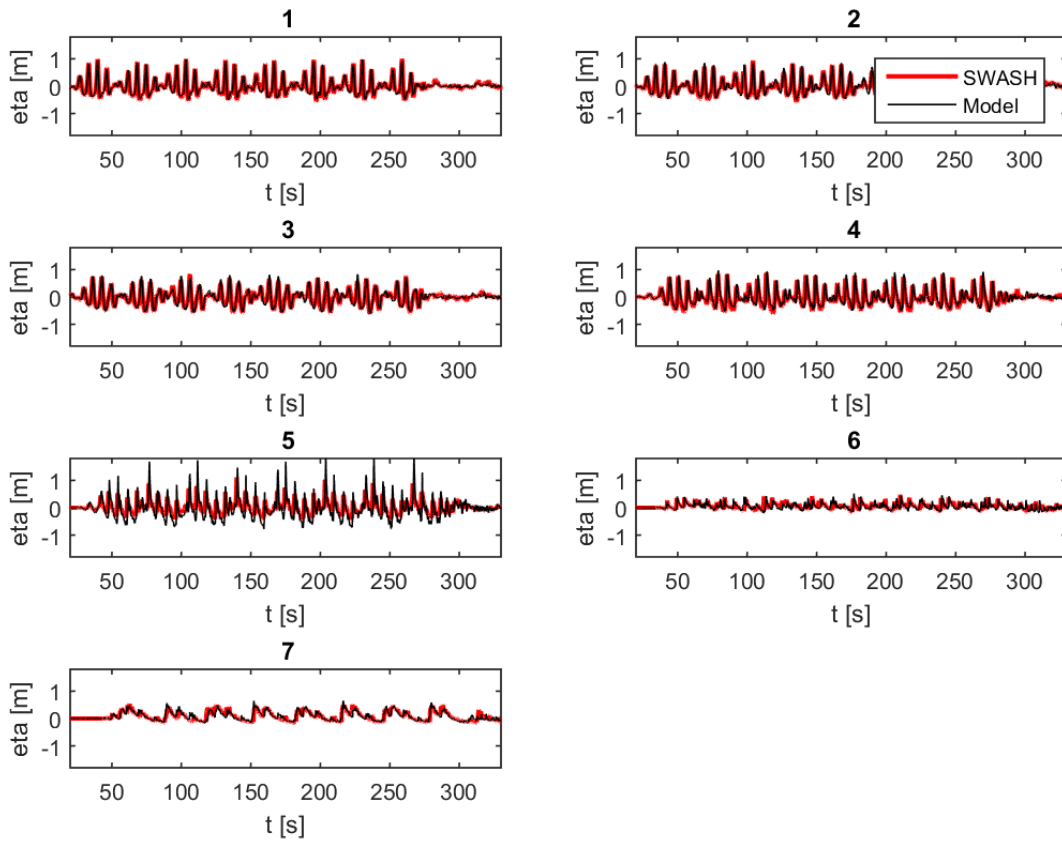
Bi\_02\_6\_R



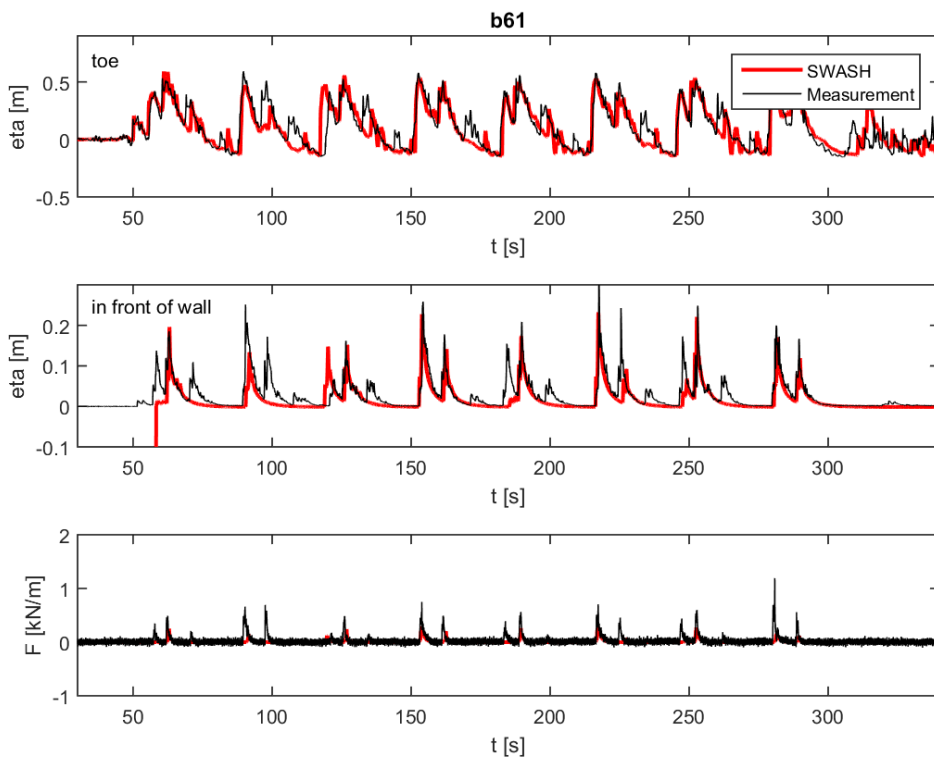
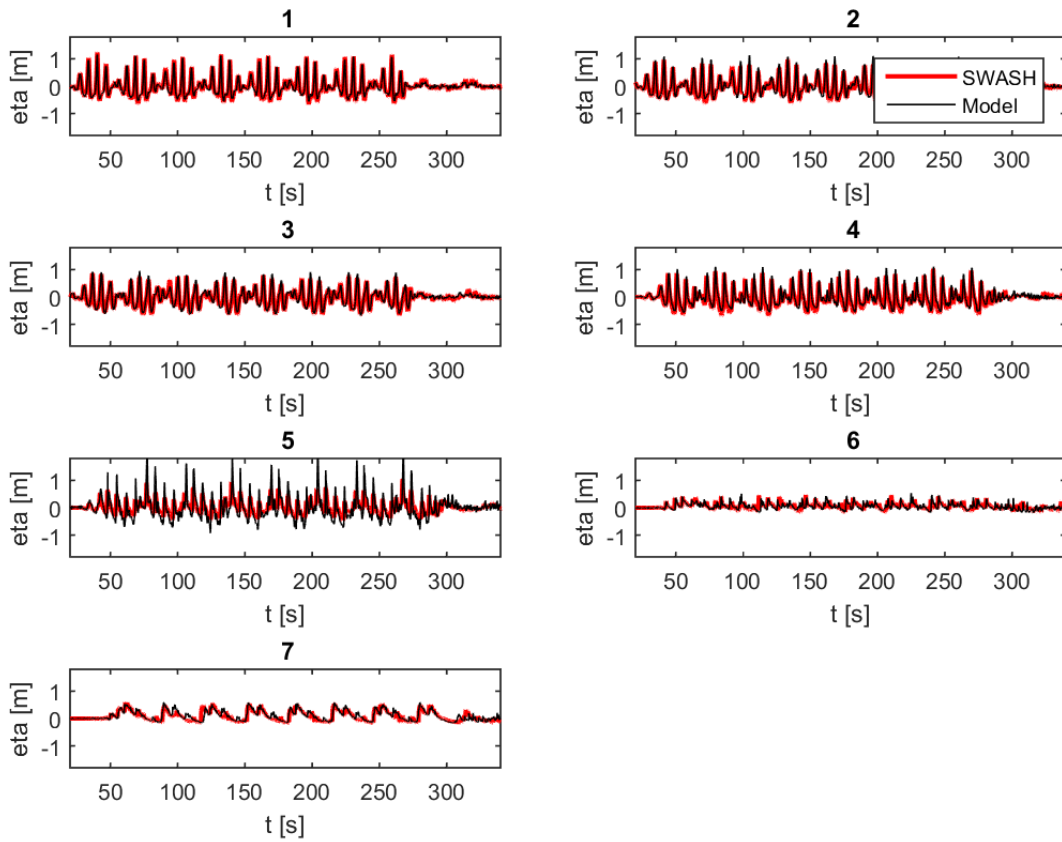
## Bi\_01\_6\_R



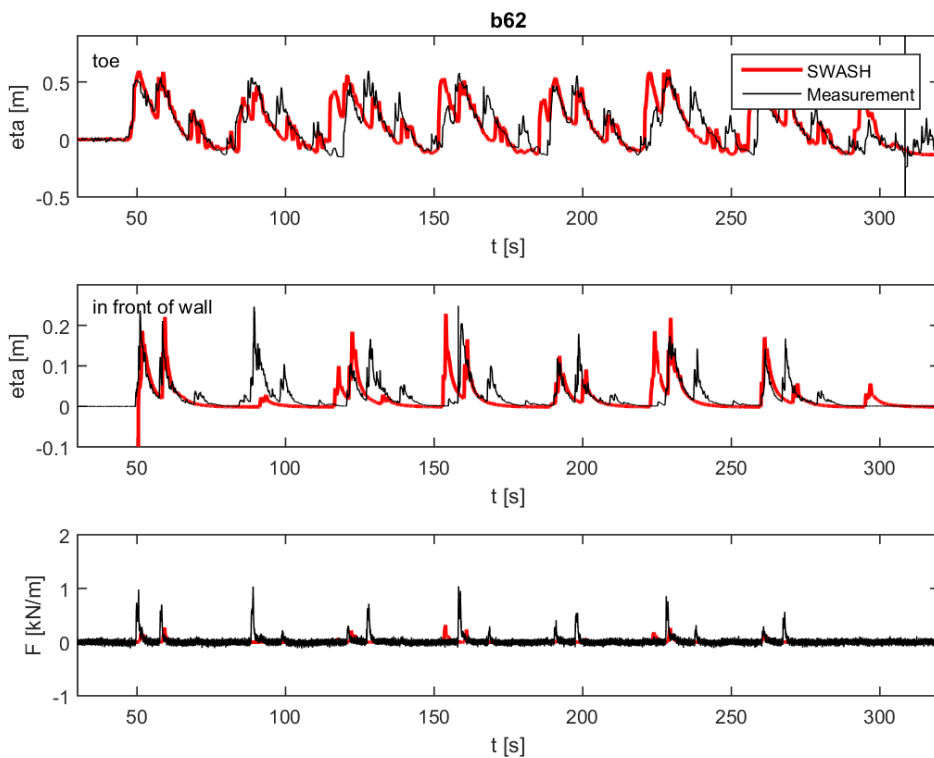
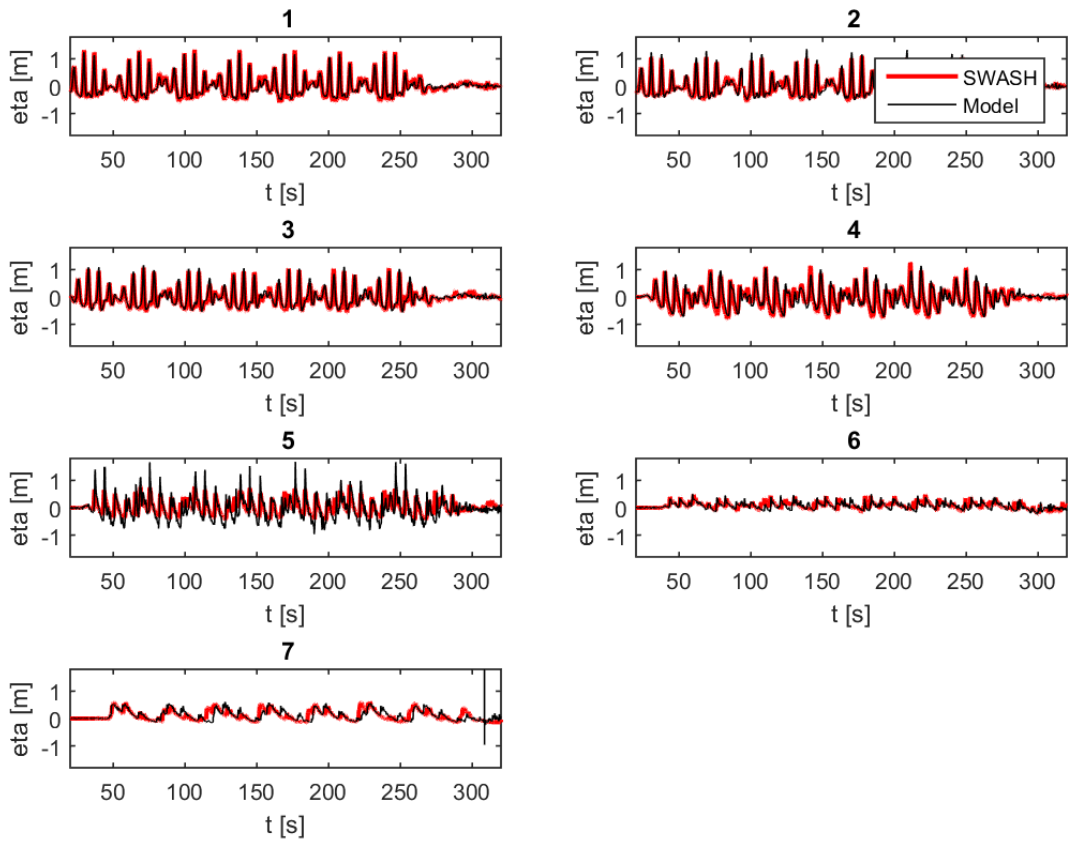
Bi\_03\_6



Bi\_03\_6\_1



Bi\_03\_6\_2



## Appendix B: Test case calculation

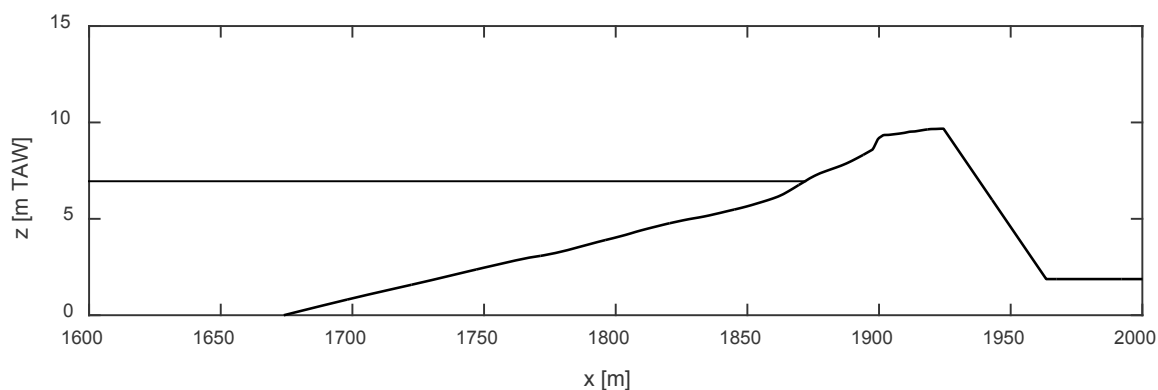
The proposed methodology is tested for the cross section 233 (XB raai 140) and 234 (XB raai 145) (cfr. 16\_027 Knokke beach nourishment project, Table 3 at p.25 in Van Santen et al., 2017).

### Cross section 233 (XB raai 140)

The incident wave properties and overtopping discharge in the project of 16\_027 (see cross section in Figure B-1) are:

$H_s=1.11$  m ;  $T_m-1,0=47.3$  s; mean water level at the toe (SWL+setup)=7.20 m TAW and  $q=5.85$  l/s/m

Figure B-1: Bathymetry for the overtopping calculation



This test is repeated:

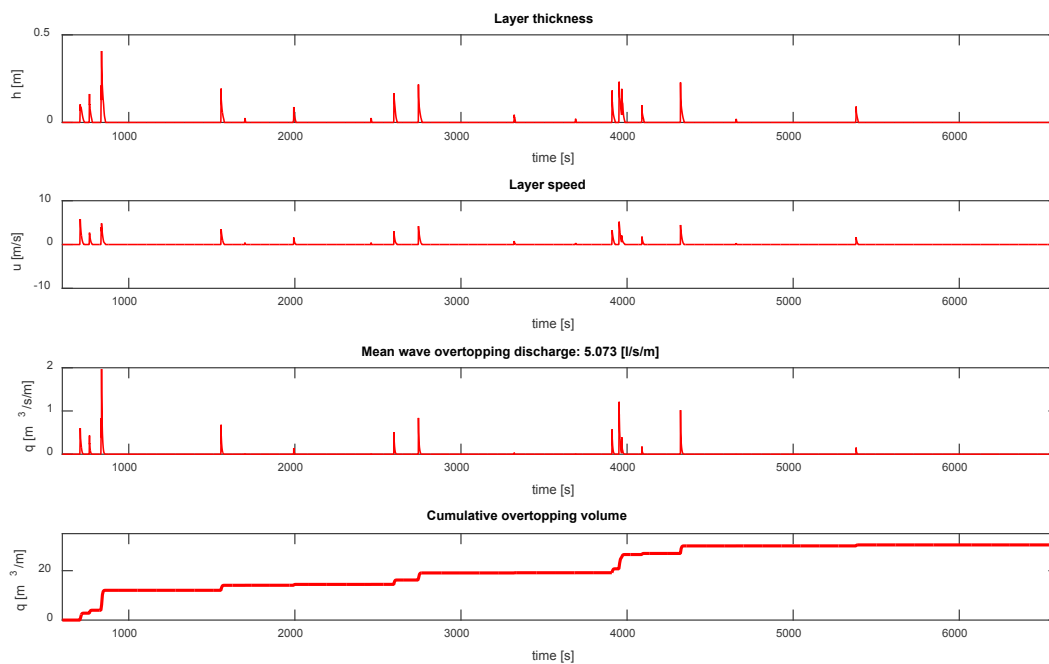
Calibration (input: SWL=7.02 m TAW,  $H_{m0}=3.27$  m,  $T_p=10.9$  s) with  $n=0.000$  using the same random number

$H_{m0}=1.10$  m (-1 %),  $T_{m-1,0}=48.03$  s (+2%) and  $h=7.02+0.125=7.15$  m (-5 cm)

Overtopping discharge

$q=5.07$  l/s/m

Figure B-2: Time series of the repeated overtopping calculation with  $n=0.000$



The incident wave properties are within the acceptable range and therefore the incident waves are fine. Overtopping discharge is slightly underestimated (-13%). The difference can be due to the difference of the SWASH version (SWASH version 4.01.A is used here). See details of this discussion in De Roo (2017).

The incident wave calibration is conducted using the bottom friction  $n=0.019$ , as proposed in Chapter 6. The results are as follows.

Calibration 1 (SWL=7.05 m TAW,  $H_{m0}=3.28$  m,  $T_p=10.9$  s) with  $n=0.019$

$H_{m0}=1.10$  m (+1%),  $T_{m-1,0}=39.04$ s(-11%) and  $h=7.05+0.196=7.25$ m (+6 cm)

-> the wave period is underestimated and water level is overestimated.

Calibration 2 (SWL=6.95 m TAW,  $H_{m0}=3.40$  m,  $T_p=10.93$  s) with  $n=0.019$

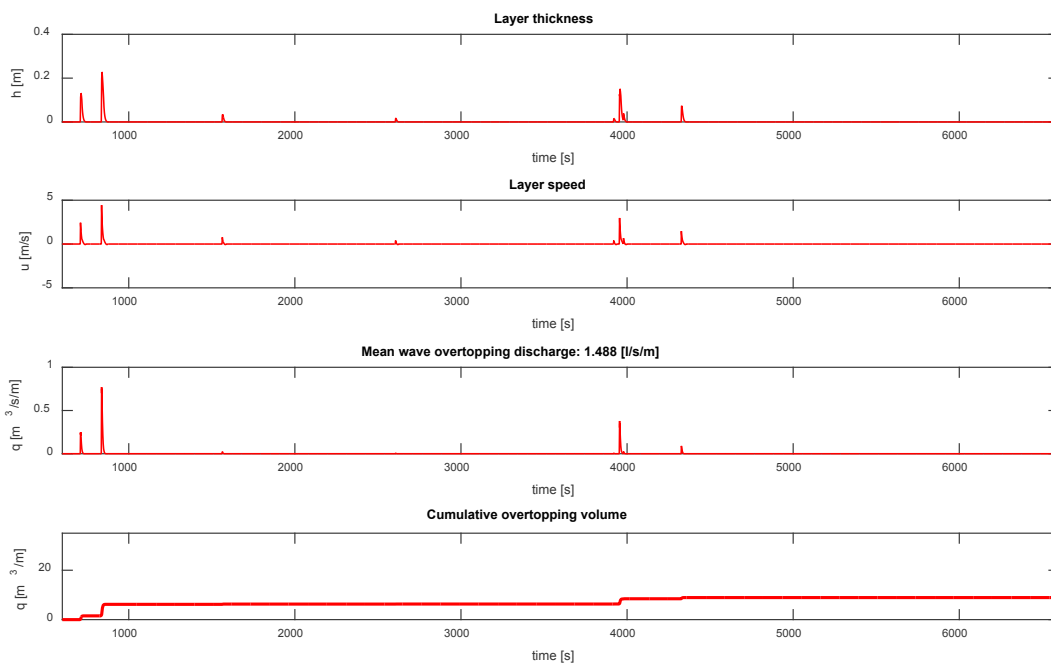
$H_{m0}=1.10$  m (-1%),  $T_{m-1,0}=46.0$  s(-3%) and  $h=6.95+0.239=7.19$ m (-2 cm)

-> all the parameter is within the acceptable range.

The overtopping calculation is conducted and the result is shown below.

$q = 1.49$  l/s/m

Figure B-3: Time series of the overtopping calculation with  $n=0.019$



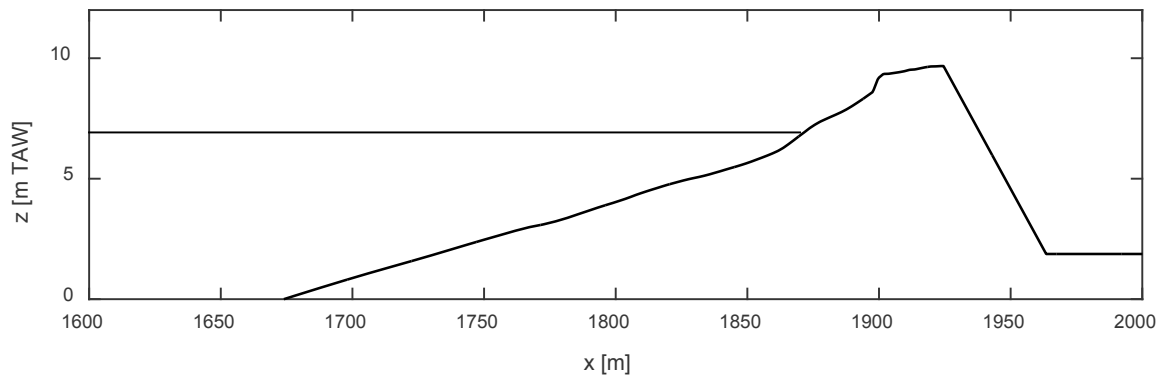
As can be seen in the figure, the smaller overtopping events are disappeared. The average overtopping discharge is lowered around 30% compared to the original one (i.e. 1.49 from 5.14 l/s/m).

## Cross section 234 (XB raai 145)

The incident wave properties and overtopping discharge in the project of 16\_027 (see cross section in Figure B-1) are:

$H_s=1.09$  m ;  $T_{m-1,0}=43.8$  s; mean water level at the toe (SWL+setup)=7.19m TAW and  $q=6.80$  l/s/m

Figure B-4: Bathymetry for the overtopping calculation



This test is repeated:

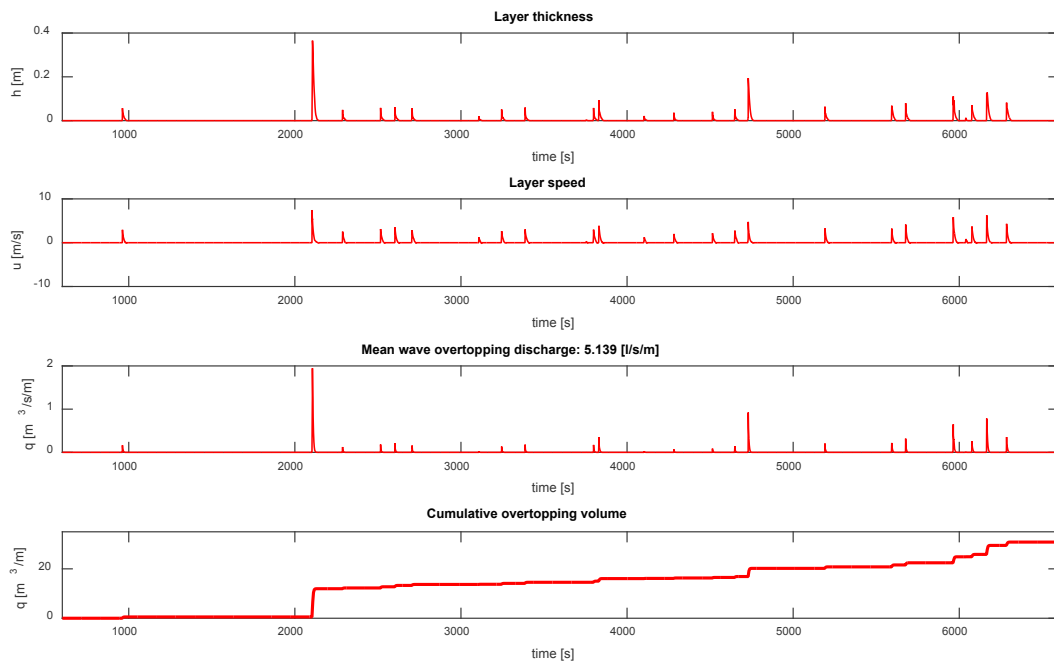
Calibration (input: SWL=7.05 m TAW,  $H_{m0}=3.28$  m,  $T_p=10.90$  s) with  $n=0.000$  using the same random number

$H_{m0}=1.09$  m (0 %),  $T_{m-1,0}=43.12$ s(-2%) and  $h=7.05+0.109=7.16$ m (-3 cm)

Overtopping discharge

$q=5.14$  l/s/m

Figure B-5: Time series of the repeated overtopping calculation with  $n=0.000$



The incident wave properties are within the acceptable range and therefore the incident waves are fine. Overtopping discharge is slightly underestimated (-24%).

The incident wave calibration is conducted using the bottom friction  $n=0.019$ , as proposed in Chapter 6. The results are as follows.

Calibration 1 (SWL=7.05 m TAW,  $H_{m0}=3.28$  m,  $T_p=10.90$  s) with  $n=0.019$

$H_{m0}=1.10$  m (+1%),  $T_{m-1,0}=39.04$ s(-11%) and  $h=7.05+0.196=7.25$ m (+6 cm)

-> the wave period is underestimated and water level is overestimated.

Calibration 2 (SWL=6.91 m TAW,  $H_{m0}=3.45$  m,  $T_p=10.90$  s) with  $n=0.019$

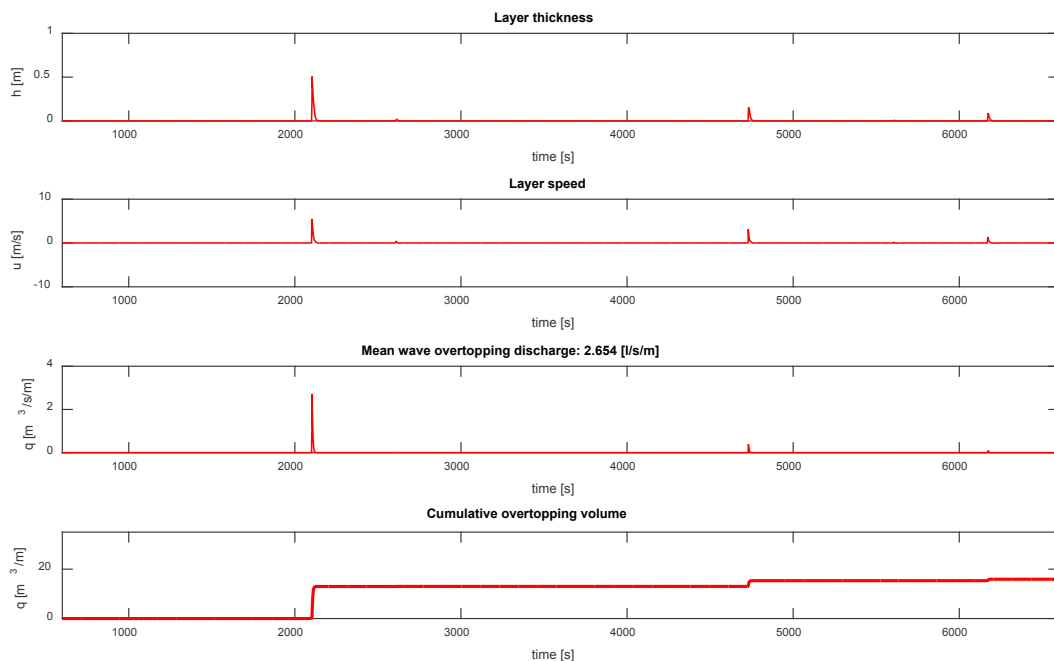
$H_{m0}=1.09$  m (0%),  $T_{m-1,0}=42.7$  s(-2%) and  $h=6.91+0.259=7.17$ m (-2 cm)

-> all the parameter is within the acceptable range.

The overtopping calculation is conducted and the result is shown below.

$q=2.65$  l/s/m

Figure B-6: Time series of the overtopping calculation with  $n=0.019$



As can be seen in the figure, the smaller overtopping events are disappeared but still big overtopping event is less affected by the bottom friction. The average overtopping discharge is lowered around half compared to the original one (i.e. 2.65 from 5.14 l/s/m) but the cumulative overtopping volume of the first big overtopping event (around  $t=2100$  s) is not reduced (both around 12 m<sup>3</sup>/m) in this case.

DEPARTMENT **MOBILITY & PUBLIC WORKS**  
Flanders hydraulics Research

Berchemlei 115, 2140 Antwerp

**T** +32 (0)3 224 60 35

**F** +32 (0)3 224 60 36

[waterbouwkundiglabo@vlaanderen.be](mailto:waterbouwkundiglabo@vlaanderen.be)

[www.flandershydraulicsresearch.be](http://www.flandershydraulicsresearch.be)